Introduction to negative staining and cryo-electron microscopy

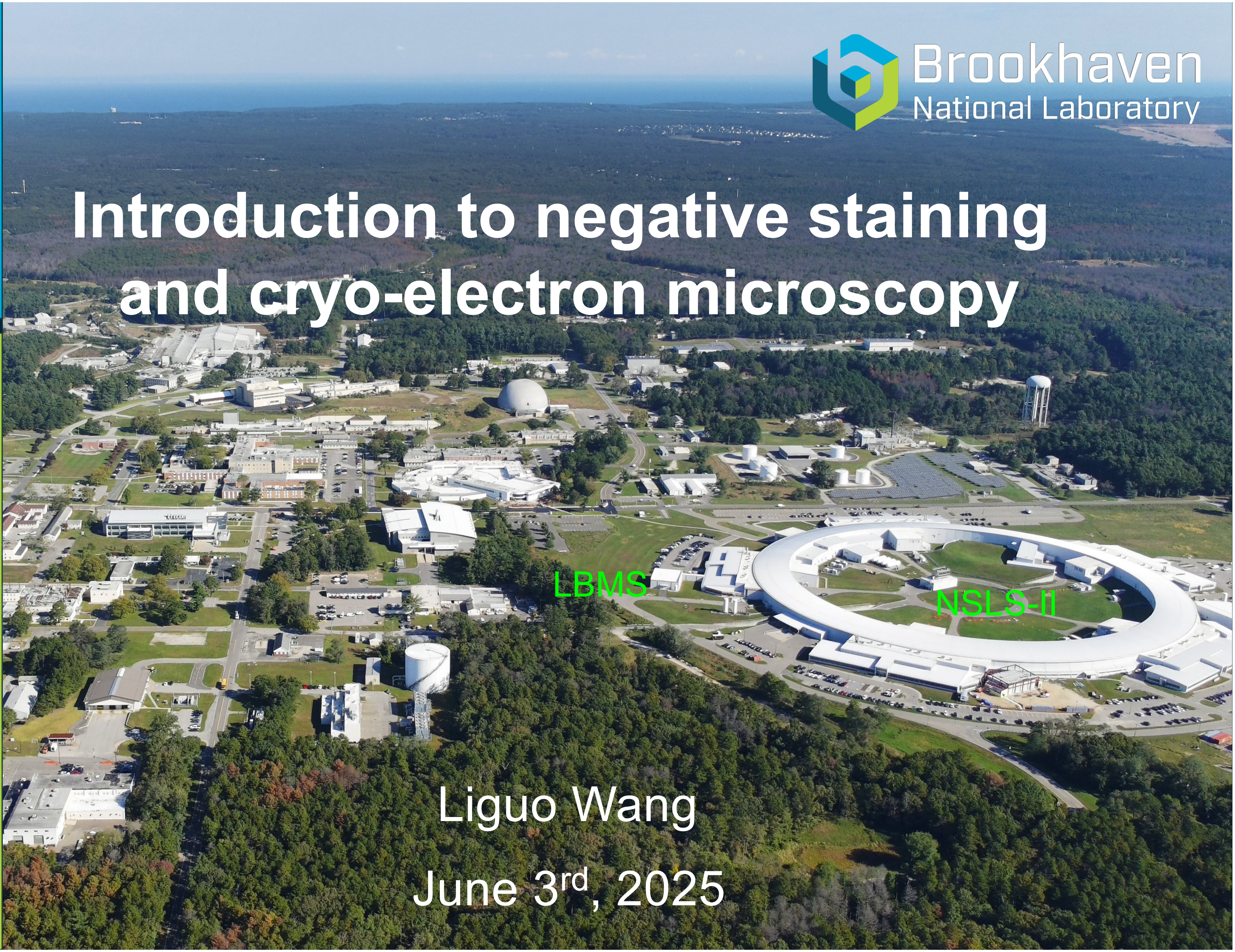

Brookhaven National Laboratory

Liguo Wang

June 3rd, 2025

Negative staining

EM requires a vacuum - an environmental constraint that is incompatible with unprotected biological material.

BSV stained with 1% 12 PTA (Phosphotungstic acid) at pH 7.0 followed by 1% 12PTA at pH 0.7

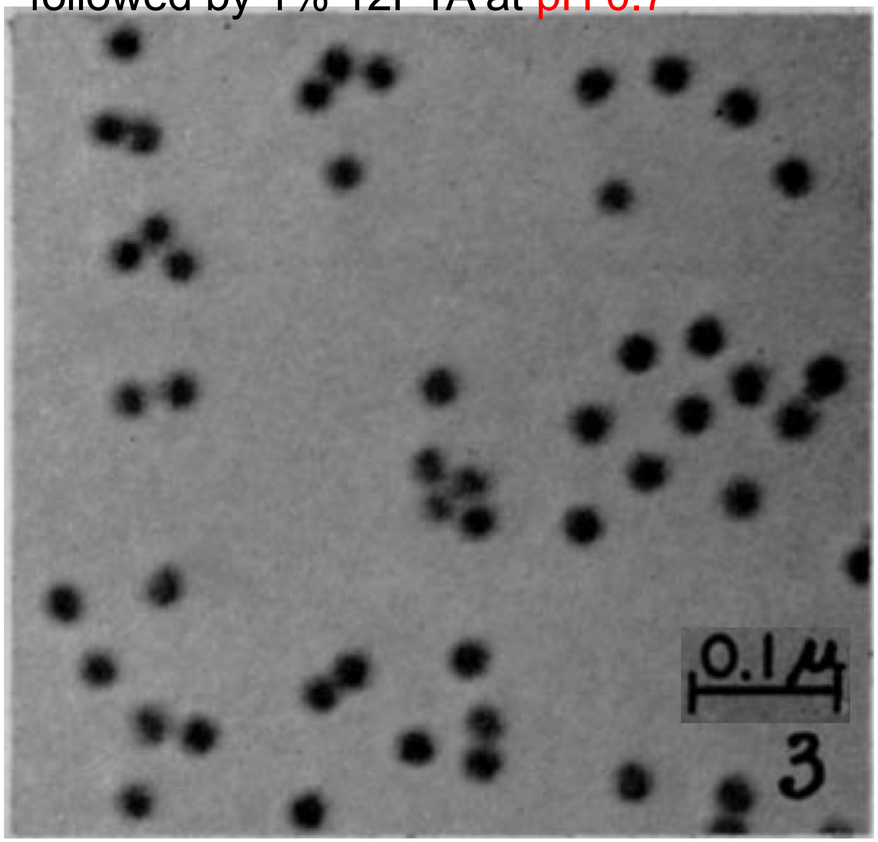

BSV stained very lightly with 5% PTA at pH 4.6 and insufficiently washed

100nm

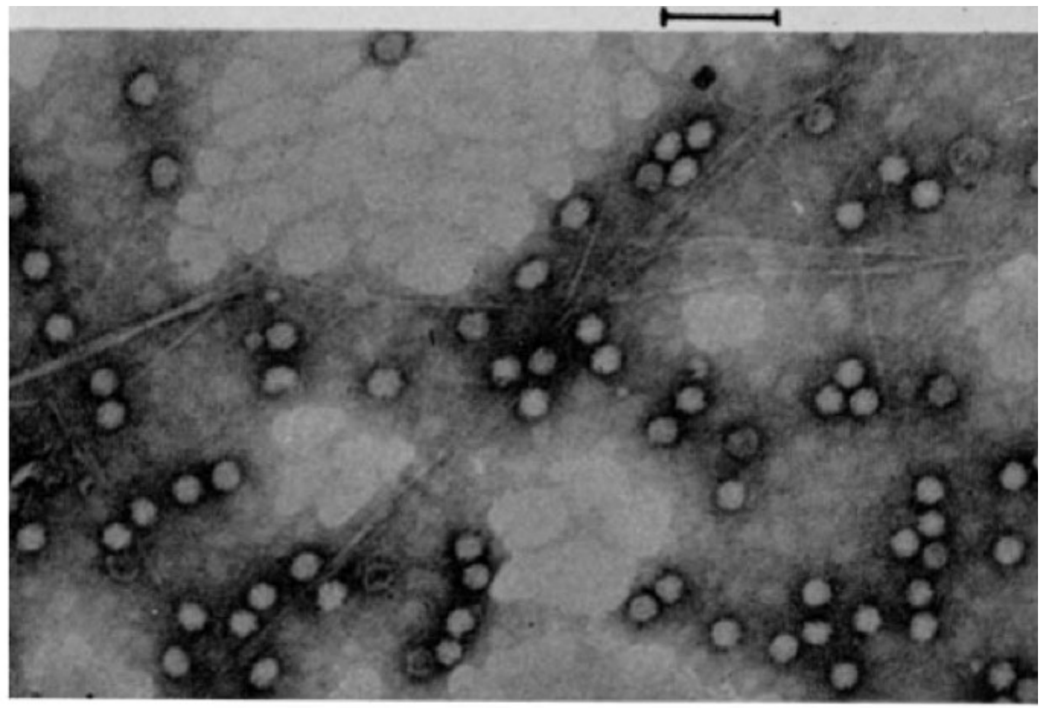

In the **pH range above 2** where the **tomato bushy stunt (BSV) viruses** are stable, the amount of stain absorbed is too small to produce adequate contrast in the electron microscope. Maximum stain absorption was achieved at pH about 1.

Hall, C. E. (1955). ELECTRON DENSITOMETRY OF STAINED VIRUS PARTICLES. The Journal of Biophysical and Biochemical Cytology, 1(1), 1-12.

Negative staining

Negative staining exploits that salts of heavy metals are relatively insensitive towards electrons and form **a stable "cast" around the molecules** when dried down. Salts such as uranyl acetate or phosphotungstic acid titrated to neutral pH, vanadates and molybdates have and are still being used.

- Sample appears "white" and the electron-dense stain is "black".
- Helps to reduce dehydration and radiation damage effects.
- Attainable resolution is ~ 15-25 Å due to clumps of stain and drying/flattening artifacts.

➔ Mainly used as a sample screening method.

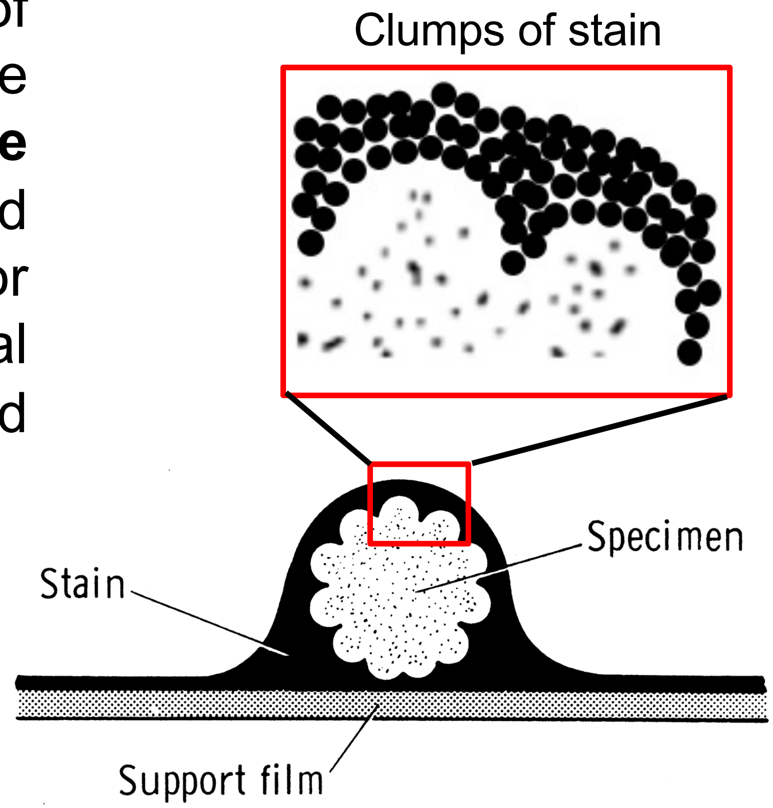

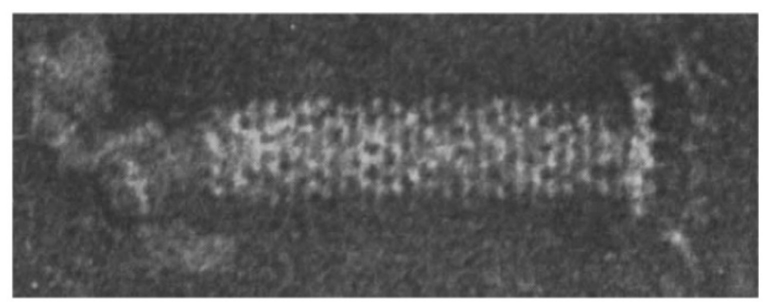

De Rosier, D.J. and A. Klug. Nature, 1968
Hayat & Miller (1990), *Negative Staining*

Radiation damage

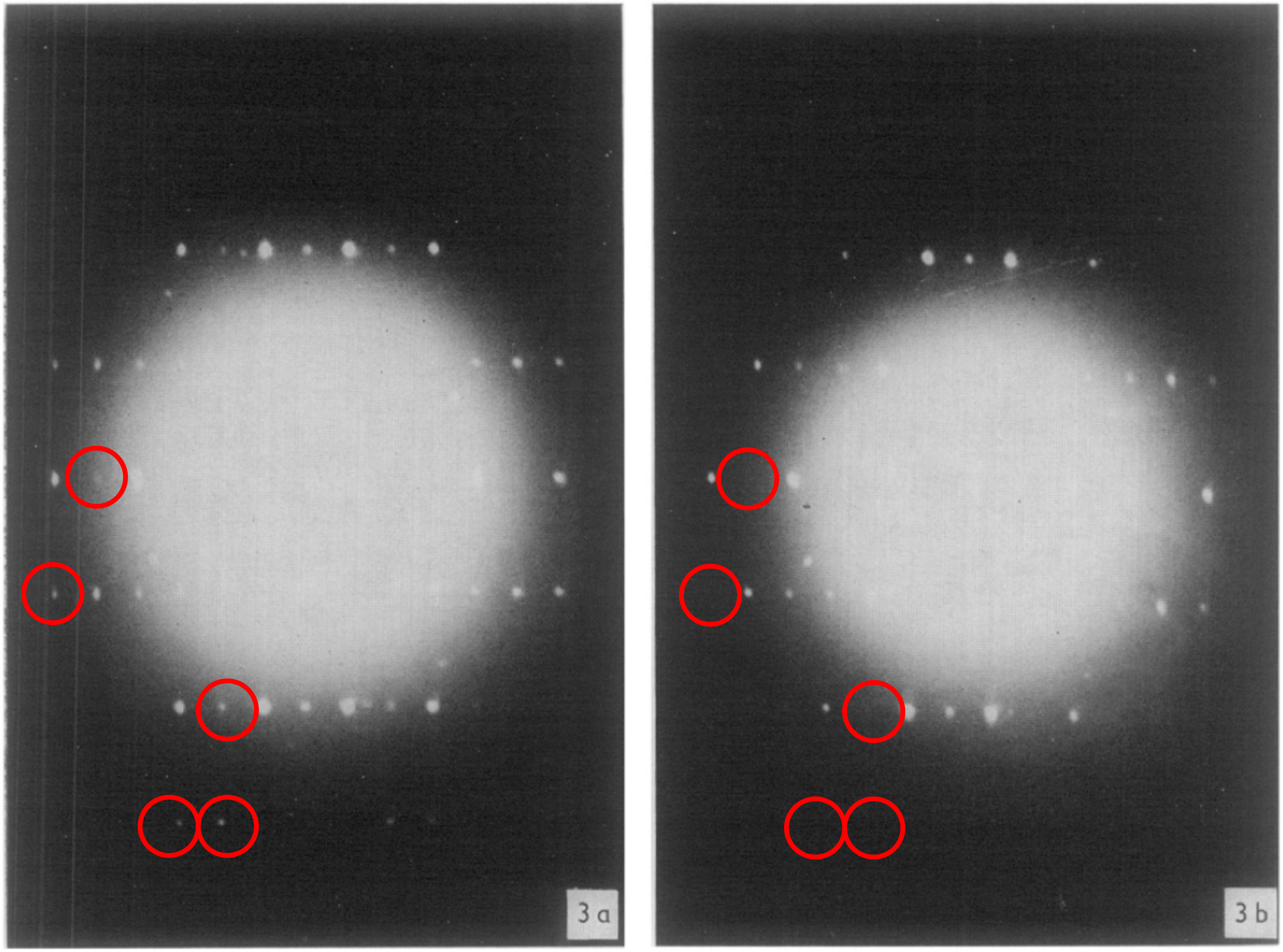

FIG. 3. The diffraction pattern of uranyl-acetate stained catalase is shown (a) before any significant changes have occurred and (b) after irradiating to a degree that no further changes occur. Reflections at Bragg spacings of less than 25 Å to 30 Å are no longer visible after so extensive an irradiation. Data were taken at 75 kV by the three-lens method (7) from a field approximately 10 μ in diameter.

Glaeser, R. M. (1971). Journal of Ultrasructure Research 36(3-4): 466-482.

Electron Diffraction of Frozen, Hydrated Protein Crystals

Abstract. *High-resolution electron diffraction patterns have been obtained from frozen, hydrated catalase crystals to demonstrate the feasibility of using a frozen-specimen hydration technique. The use of frozen specimens to maintain the hydration of complex biological structures has certain advantages over previously developed liquid hydration techniques.*

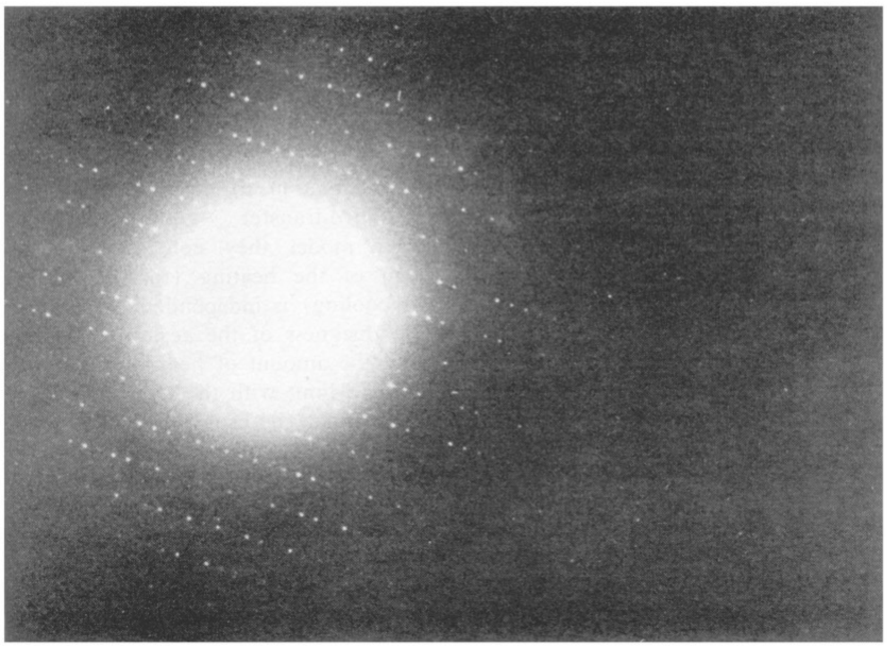

Fig. 1. Electron diffraction pattern of a catalase crystal which was frozen in liquid nitrogen and observed on a specimen stage cooled with liquid nitrogen. The resolution of the photographic reproduction is 4.5 Å, although that of the diffraction pattern on the original plate was 3.4 Å.

13 December 1974, Science 186:1036-37

In parallel to the work of Henderson and Unwin, Taylor and Glaeser discovered that biological specimen can be observed in a **frozen-hydrated state.** This discovery was not only key to advancing 2D-crystallography (and later being adopted by the X-ray community as well), but also made possible the study of single particles of large macromolecular complexes.

What does “frozen-hydrated” mean? It means that the sample is preserved in water!

How was it achieved?

Radiation damage and low temperature imaging

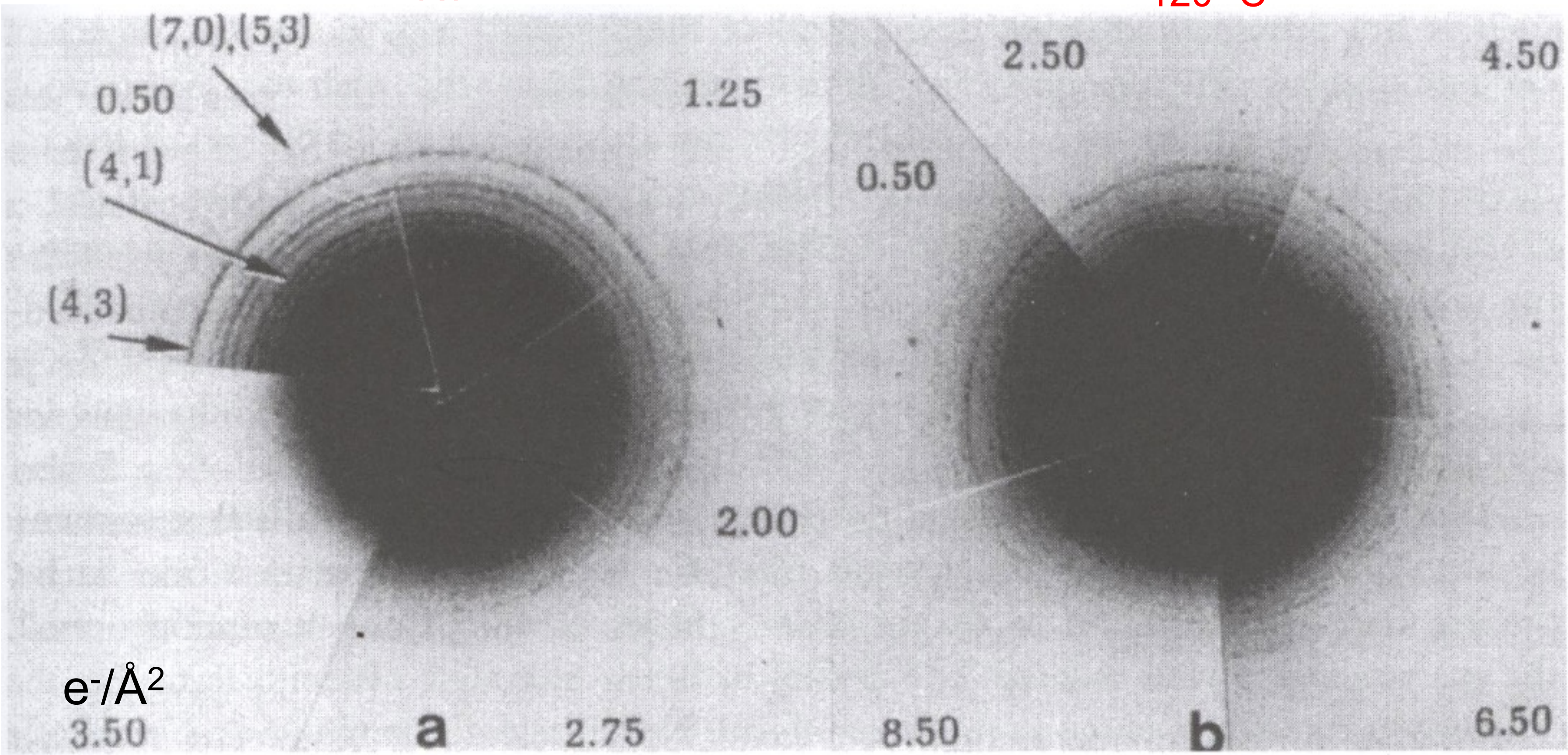

Figure 1.8 Comparison of the rate of fading of electron diffraction intensities at room temperature and at low temperature. A series of electron diffraction powder patterns of glucose-embedded purple membrane were recorded after specified periods of previously accumulated electron exposure (Hayward and Glaeser, 1979). The results show that about 5 to 7 times greater electron exposure can be tolerated at low temperature than at room temperature, for the same extent of specimen damage.

Sample is preserved in water!

Vitrification of water

- Idea was proposed in late 1930s: Father B. Luyet proposed to cool a liquid so rapidly that molecules have no time to crystallize.
- Idea was not favorable: due to the discovery of the cryoprotecting effect of glycerol, ice crystals are allowed to grow but under controlled conditions.
  ➔ The vitrification of water was thought to be fundamentally impossible.
- Rapid development in 1980-1983
  - In 1974: Taylor and Glaeser, frozen catalase crystal (a drop between two grids was blotted and plunged into liquid nitrogen)
  - In 1981, Duboche group vitrified thin water layers, obtained by spreading on a support, by immersion in liquid ethane (Dubochet & McDowall, 1981)
  - In 1983, EMBO course to teach the vitrification method.
    - Use of liquid ethane
    - Reducing the volume to be frozen

Why is liquid ethane preferred over liquid nitrogen?

	Melting Point (°C)	Boiling Point (°C)	Heat of vaporization (kJ/kg)	Heat capacity (kJ/(kg·K))	Heat to boil (kJ/kg)	Heat to evaporate (kJ/kg)	Liquid density (kg/m3)
Nitrogen	-210	-196	6	0.9-1.6	13-22	19-28	809
Ethane	-183	- 89	489	2.3-3.5	216-329	705-818	546
Water	0	100	2257	4.185	418.5	2675.5	1000

- Rapid boiling of nitrogen disrupts consistent cooling.
- Generation of a gaseous layer around the sample prevents fast cooling.

Sample Vitrification

Need high relative humidity in environment because at wind velocities of ~1m/s and 4˚C the rate of natural water evaporation is: ~52Å/second (99% humidity) but ~1000Å/second at 80% humidity. At room temperature, this rates are about 4-fold higher!

➔Decreasing sample size to increase the cooling speed.

Water drop ➔ thin layer of water, 1,000-100,000 times thinner!

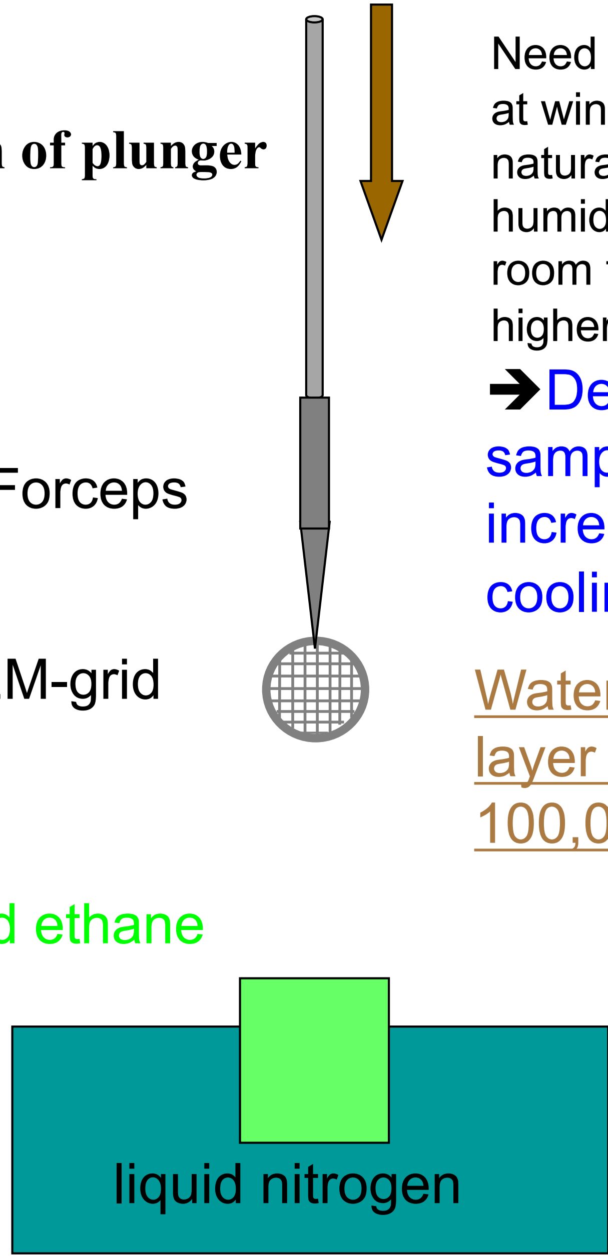

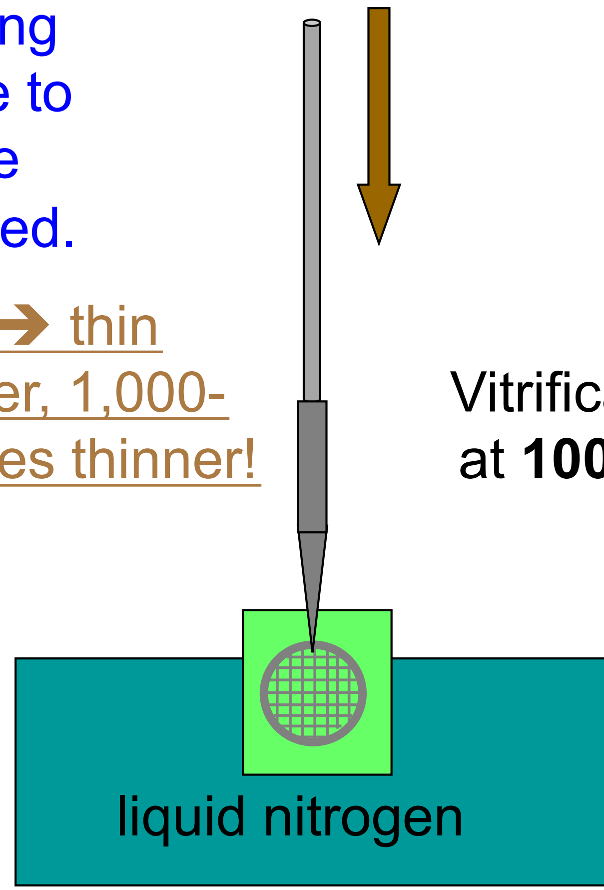

Vitrification occurs at **100,000** ˚C/sec

Cooling speed is the key for amorphous ice

- Vitreous ice:
  An amorphous solid state in which water was frozen without adopting any crystalline structure.

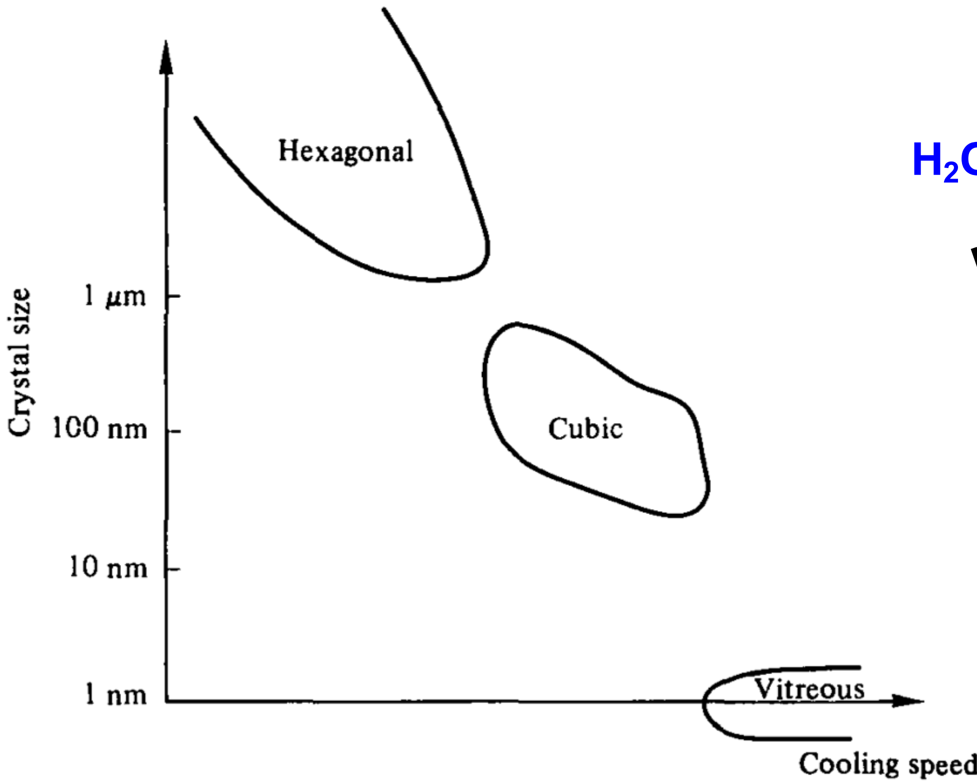

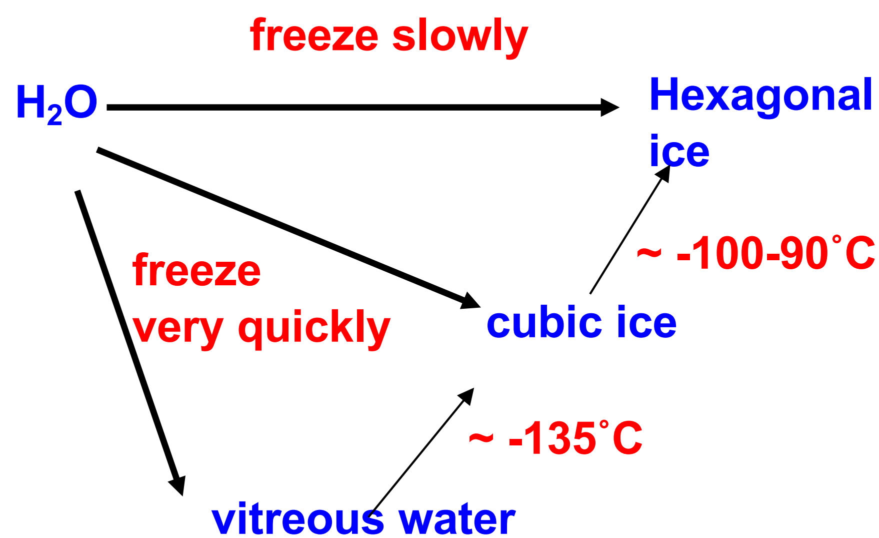

Phase transition of ice

Devitrification of vitreous ice should take place in *c.* 7 min at -137 °C

28 min at -140 °C

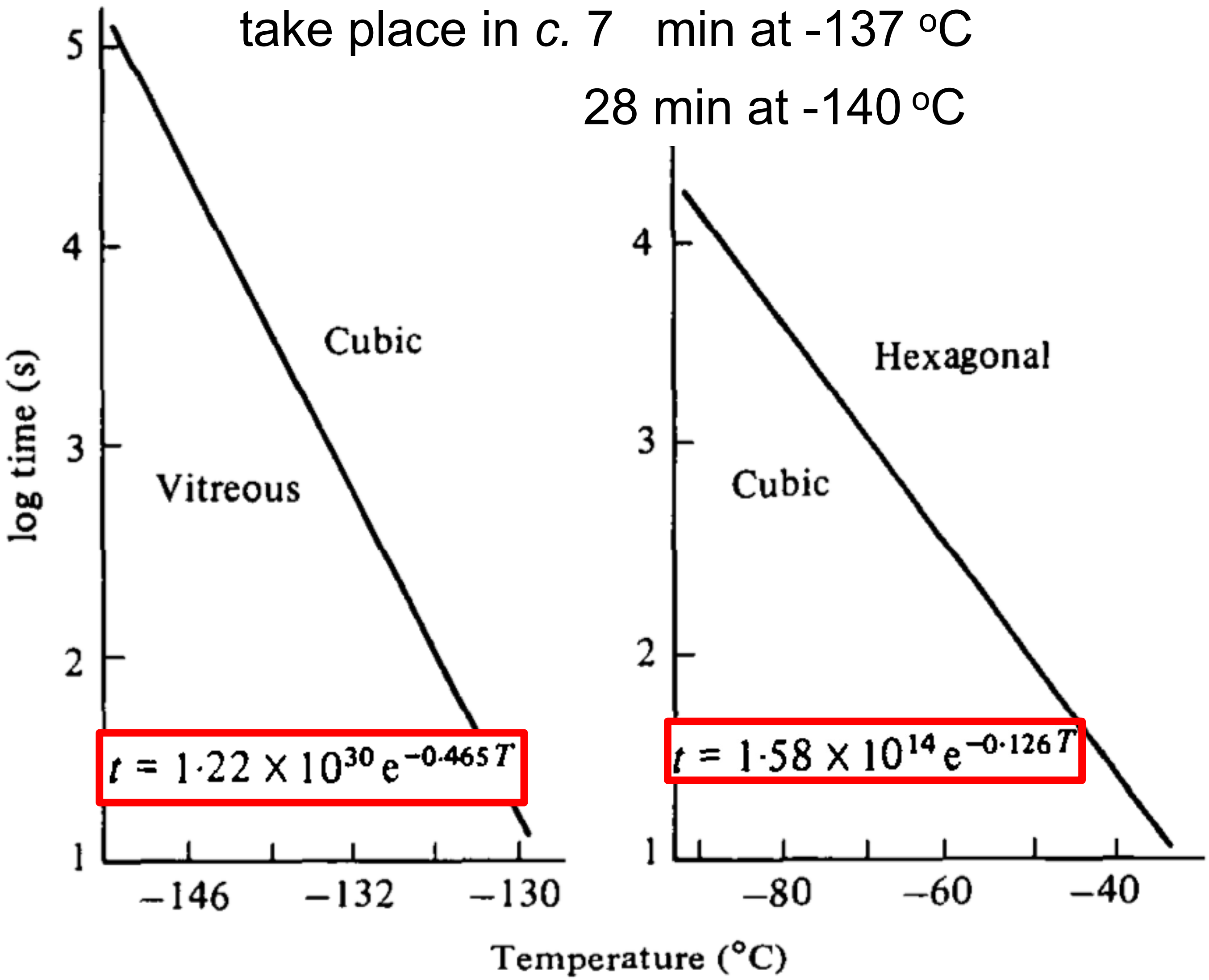

Fig. 6. Time t required, at the temperature T (° C), for the phase transition from (a) vitreous water to cubic ice and (b) cubic to hexagonal ice to take place (Dowell & Rinfret, 1960). Recent results suggest that curve (a) should be displaced by 10-20 ° C towards the higher values (see text).

Dubochet, J., Adrian, M., Chang, J. J., Homo, J. C., Lepault, J., McDowall, A. W. & Schultz, P. (1988). Cryo-electron microscopy of vitrified specimens. Quarterly Reviews of Biophysics, 21(2), 129-228.

Workflow of cryo-EM

Single Particle Analysis (SPA) of many identical copies

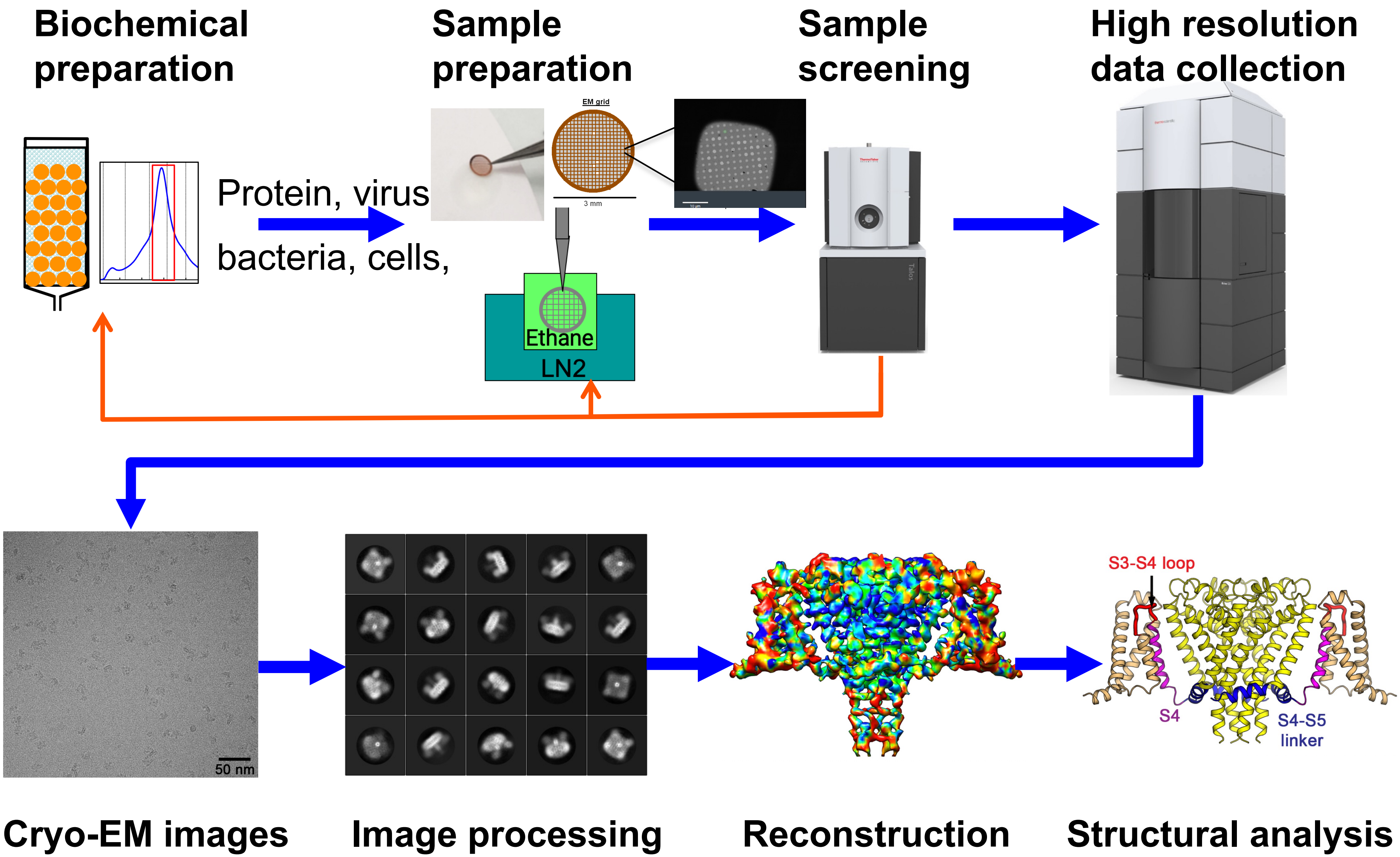

SPA cryo-EM: individual atoms are resolved!

Human Apoferritin at 1.2 Å resolution

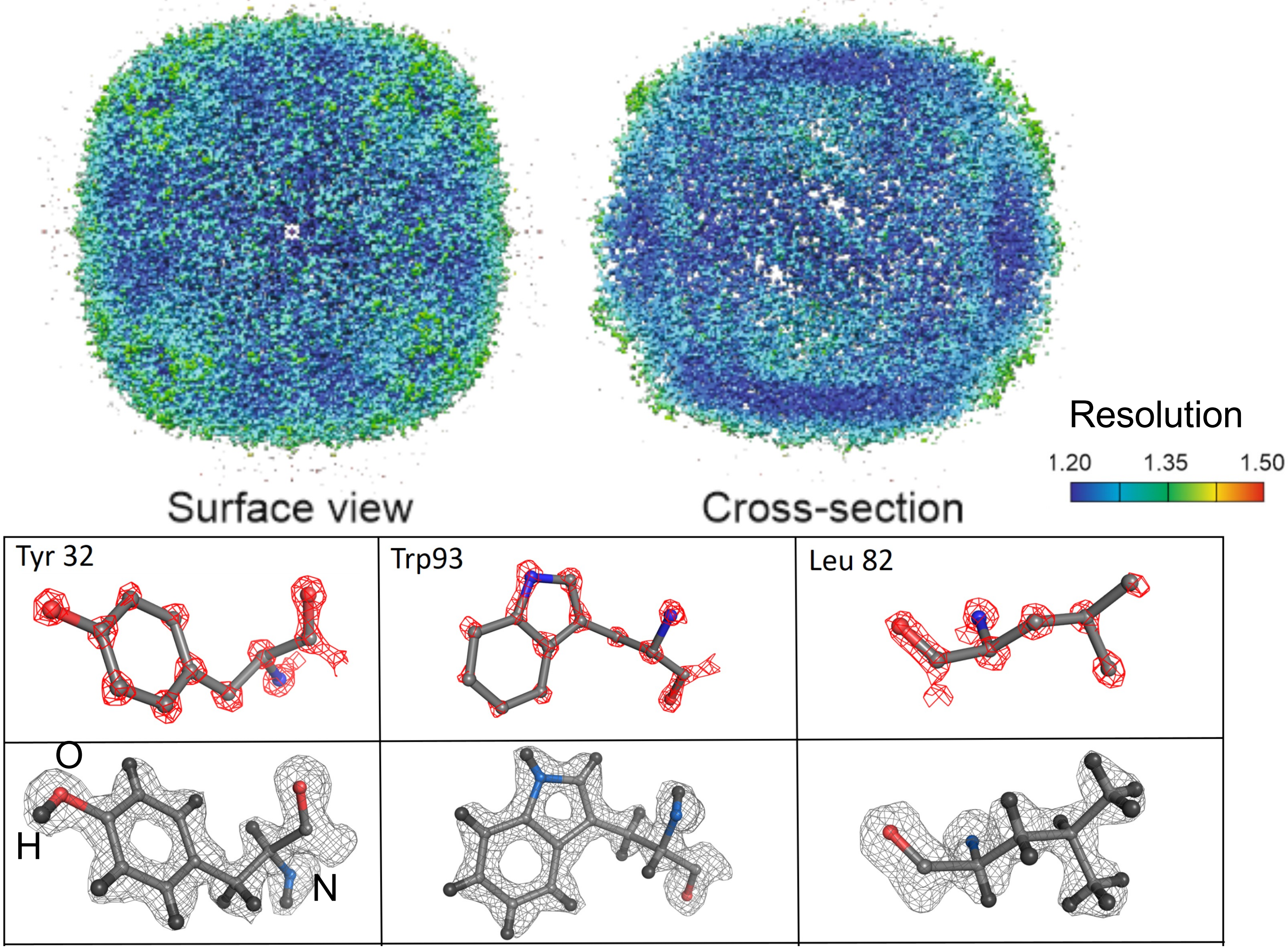

K. M. Yip et al. Preprint at bioRxiv http:// doi.org/dx3w; 2020
T. Nakane et al. Preprint at bioRxiv http://doi.org/dx3x; 2020

Sample preparation

Continuous carbon grids for negative staining

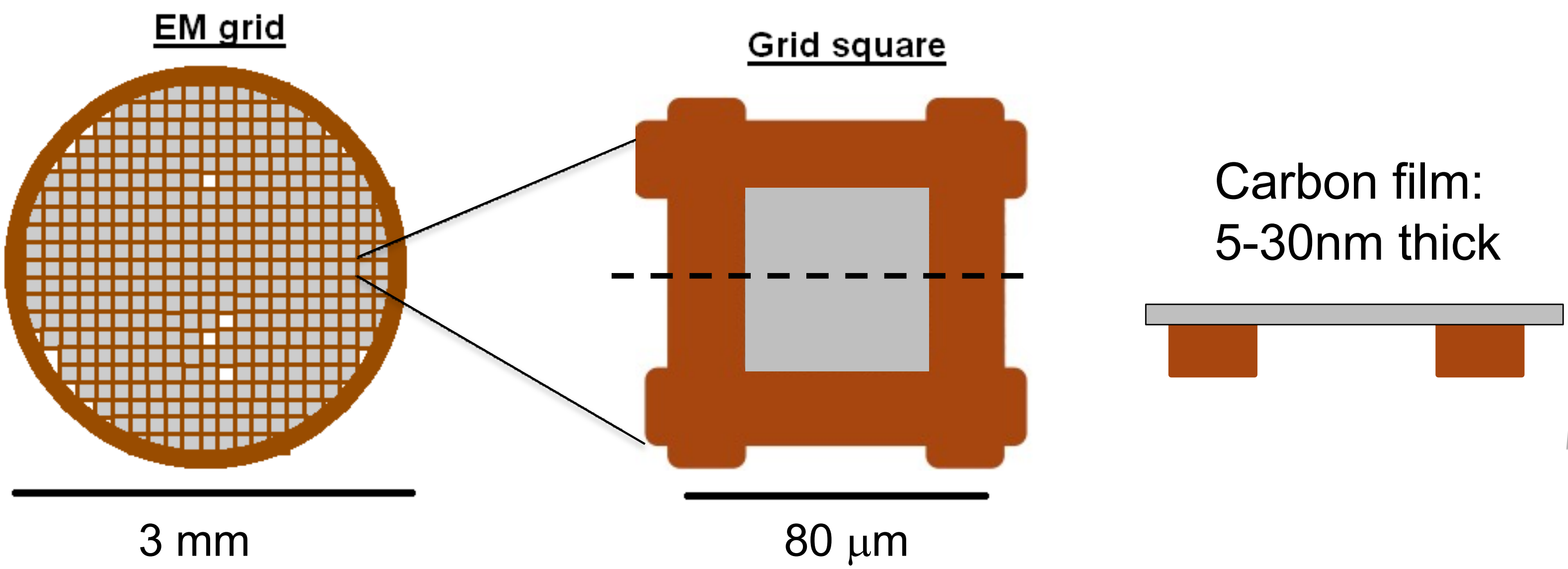

An EM grid coated with a thin **continuous carbon film** (5-30 nm).

400 mesh: 400 squares in 1 inch➔2.54cm/400=63.5 microns

- ➔ 400 mech grids are preferred
- ➔ Can be made in the lab or purchased from companies

Glow discharge to render hydrophobic carbon film to hydrophilic film

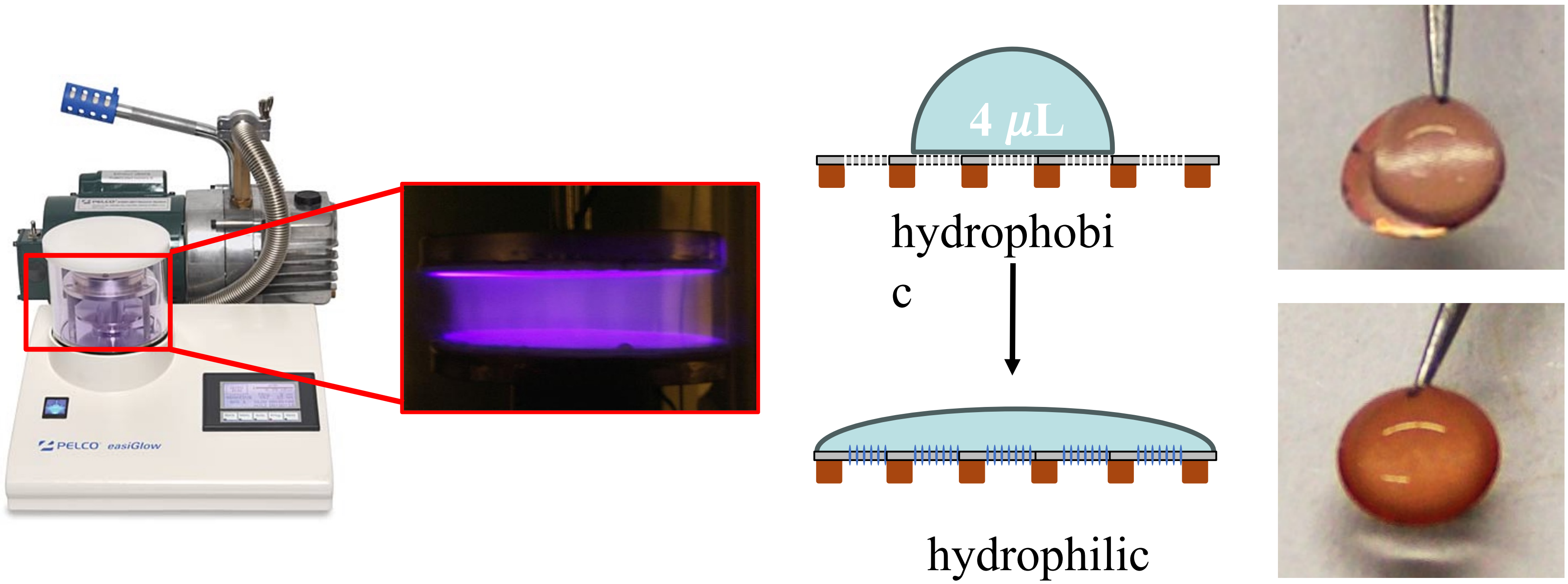

(a) (b) (c) (d)

- 20-30mA, 20 s for carbon
- 20-30mA, 120 s for gold
- 10 mA, 5s for ultrathin carbon coated holey grids

Wang, L. and C.M. Zimanyi, *Cryo-EM sample preparation for high-resolution structure studies.* Acta Crystallogr F Struct Biol Commun, 2024.

Staining solutions

Stain	Density (g/ml)	Useful pH range	Radiation sensitivity	Contrast	References	Comments
Uranyl acetate	2.89	3– 4	Moderate	High	Van Bruggen et al. [101]	Fixative effect
Uranyl oxalate	2.50–3.07 [b)]	3– 7	Moderate	High	Haschemeyer and Meyers [10]; Mellema et al. [102]	Very light sensitive, store frozen
Uranyl nitrate	2.81	3– 4	Low	High		
Uranyl formate	3.70	3– 4	Moderate	High	Haschemeyer and Meyers [10]; Leberman et al. [103]	Fixative effect, smallest grain size
Uranyl sulfate	3.28	3– 4	Low	High	Estis et al. [104]	Reported not to recrystallize upon irradiation with electrons
Na/K-phosphotungstate	1.69 [c)]	4– 9	Low	High	Brenner and Horne [105]	Positive staining, increases with lowering the pH; destructive effect on phospholipid membranes
Na silicotungstate	2.84 [d)]	4– 8	High	High	Sherman et al. [106], Terry [107] Haschemeyer [108]	
Methyl-phosphotungstate		4– 9.5	Low	Medium	Oliver [109]	
Methylamine tungstate	3.88	3–10	Low	High	Faberge and Oliver [110], Shaw and Hills [111]	Supposed not to be a positive stain at any pH. With glycoproteins, add tannic acid
Ammonium molybdate	2.28	5– 8	Moderate	Medium	Bohonek [112], Manella and Frank and [113]	Good for membranes, some fibrous proteins
Aurothioglucose	2.92	4–10	High	Low	Kühlbrandt [114], Kühlbrandt and Unwin [13]	Yields Au-crystallites upon electron irradiation
Cadmiumthio-glycerol	2.0	4–10	Moderate	Low	Jakubowski et al. [15]	No crystallite formation upon electron irradiation, possibly useful with undecagold
Vanadate	2.85 [e)]		Low	Low		Very light stain, can be used with undeca-gold labelling

Bremer, A. et al Ultramicroscopy 46 (1992) 85-111

Staining solutions

Stain	pH range	Note
Sodium (K) phosphotungstate	5-8	Significant disruptive effect on many membrane systems. Interact with lipoproteins. Less likely to precipitate with salts and biological media
Uranyl acetate (1-3%)	4.2 – 4.5	Highest electron density and image contrast
Sodium silicotungstate (1-5%)	5-8	Good contrast; Good for small particles and individual molecules
Ammonium molybdate (1-2%)	5–7	Best results for many types of specimen; Lower electron density than other stains
Methylamine tungstate (2%)	6-7	Contrast is not as good as uranyl acetate. Resolution is good.
Uranyl formate (0.75-1%)	4.2-4.5	Best for small molecules, but only stable for 1-2 days.
Nano-W® (methylamine tungstate)	6.8	Excellent spreading qualities and a high density for high contrast

Holey TEM grids for cryo-EM

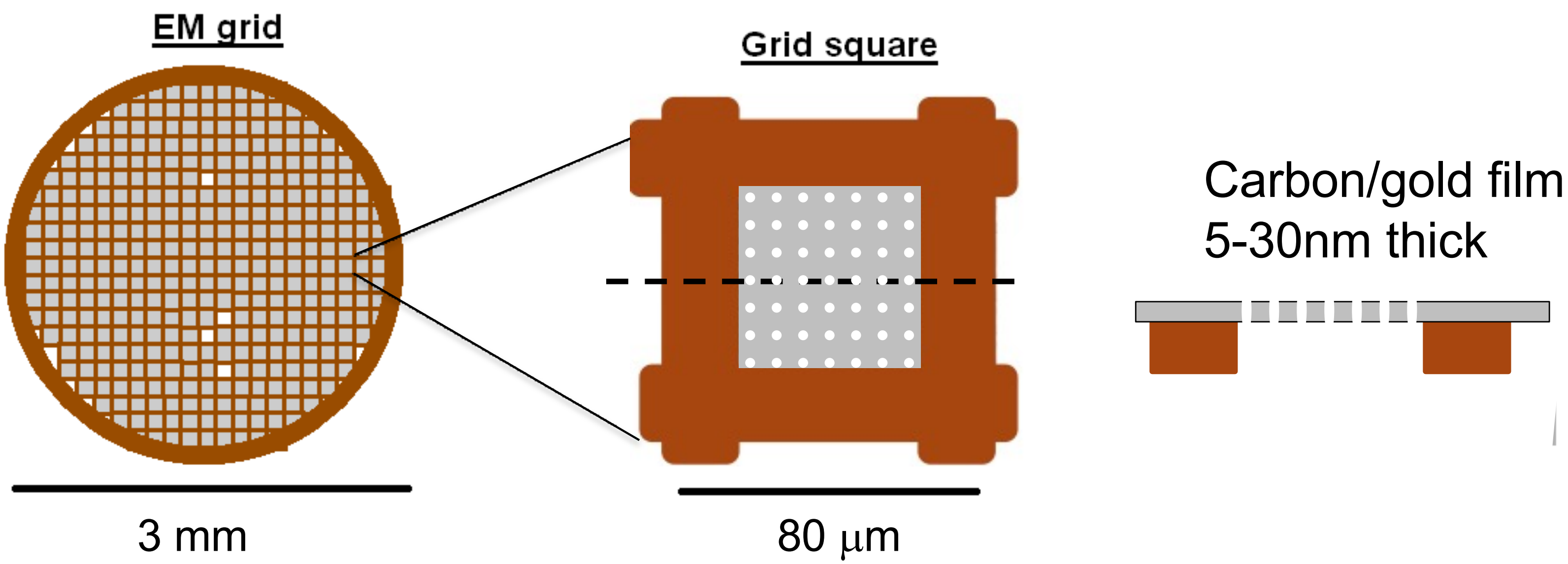

An EM grid coated with a thin carbon film (5-30 nm).

300 mesh: 300 squares in 1 inch➔2.54cm/300=84.6 microns

- ➔ 300 mech grids are preferred
- ➔ Mainly purchased from companies

Why are 300 mesh grids recommended for SAP at LBMS?

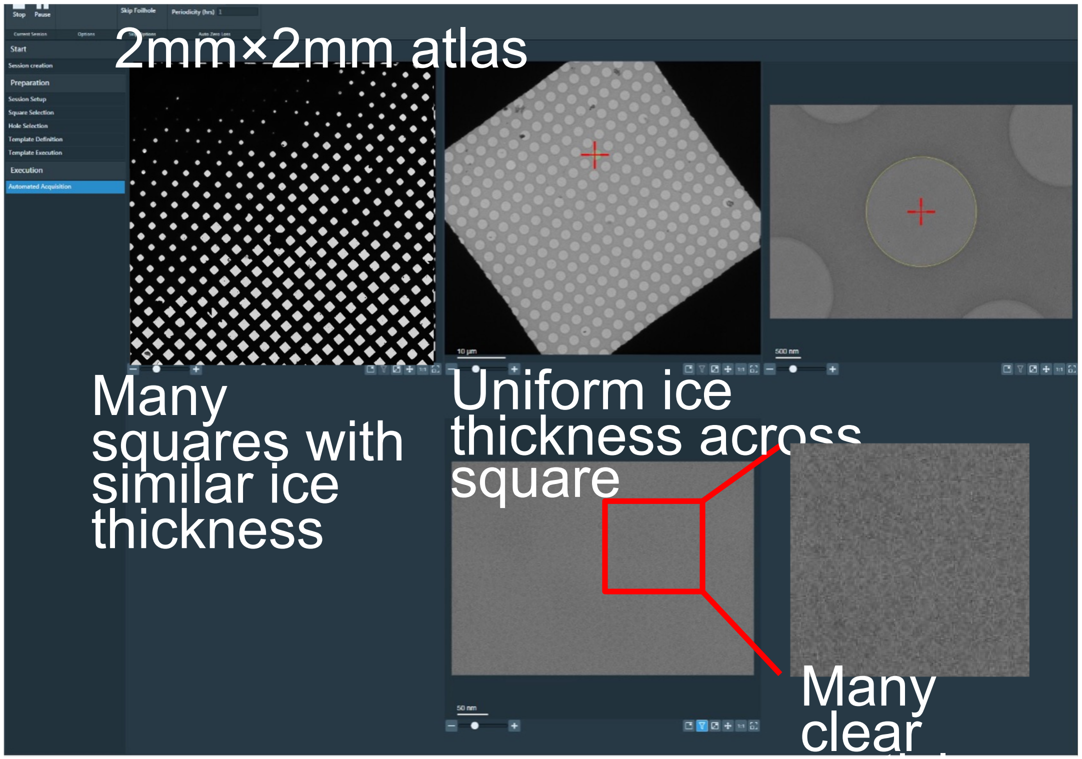

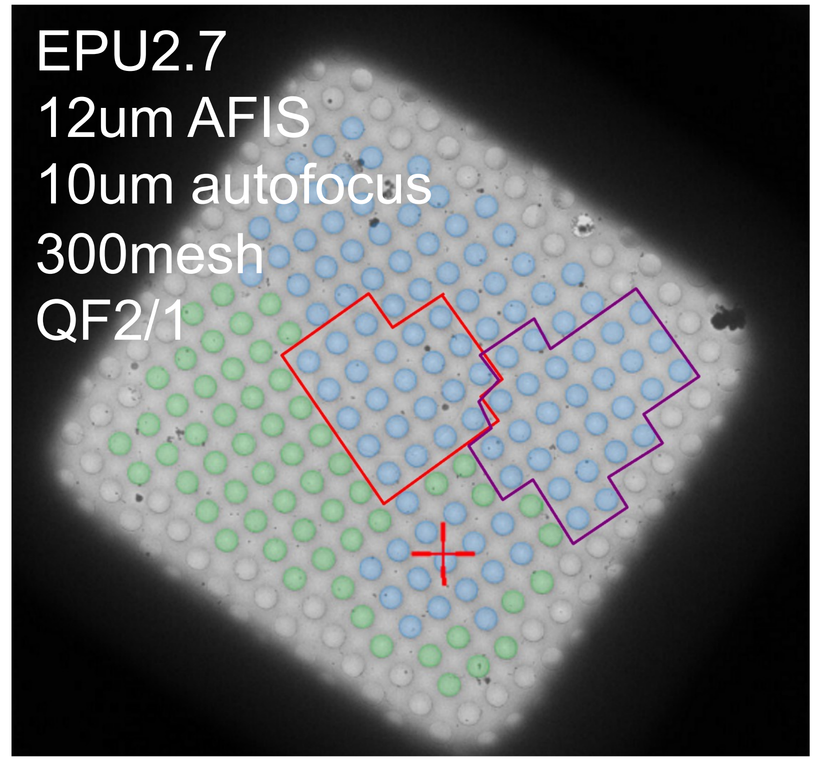

Actions for each square

- Move stage to bring it to U-Z height
- Image and select holes
- Move stage to each hole, wait for the stage to settle, image, then repeat.

Group holes and image with AFIS

- Move stage only once for each group
- Wait for the stage to settle, image all holes in this group
- Repeat for another group

Why are automated plungers preferred over manual plungers?

- Reproducibility and Consistency
- Controlled Environmental Conditions

Controlled conditions to control water evaporation

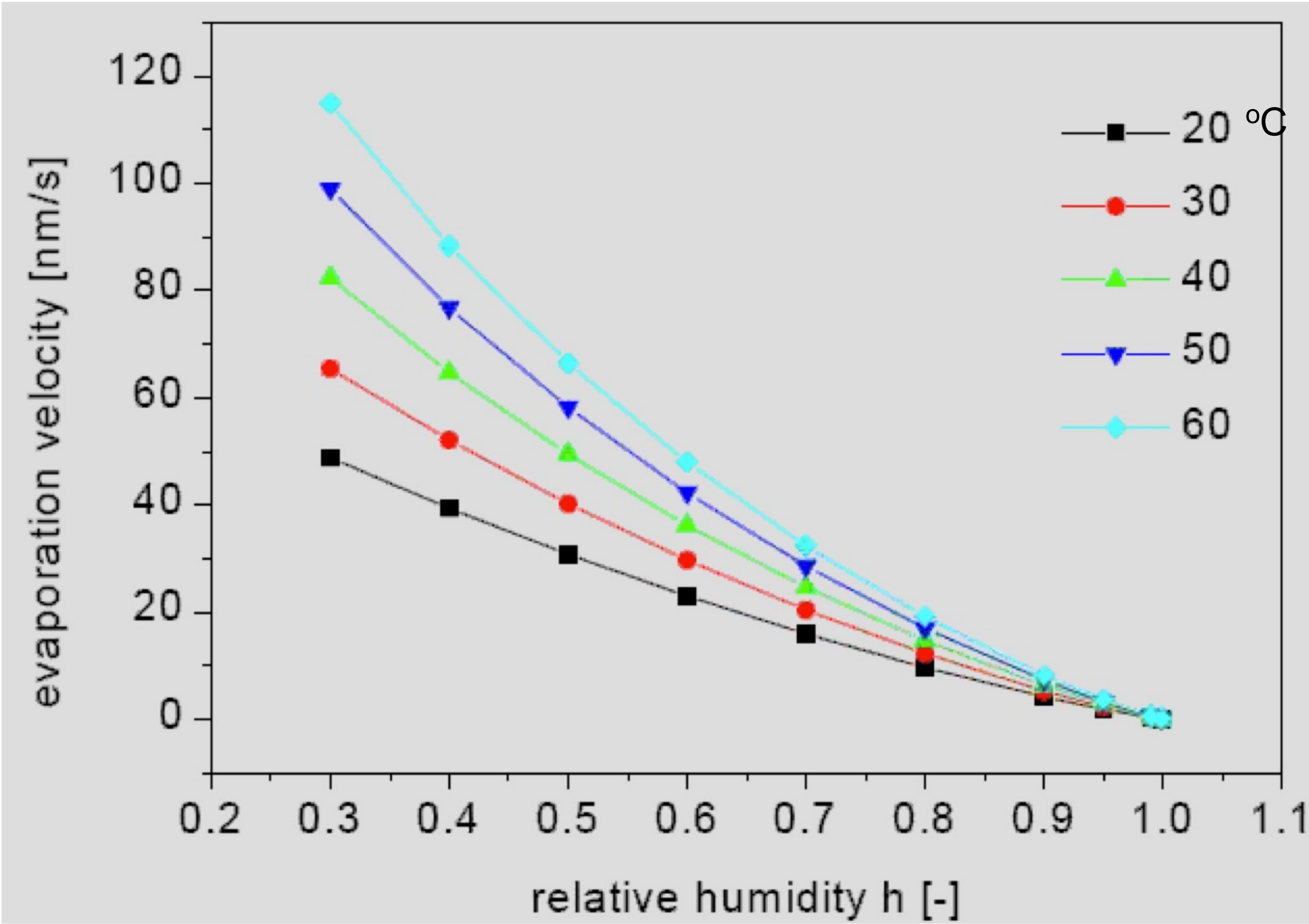

Frederik, P.M. and D.H.W. Hubert, *Cryoelectron Microscopy of Liposomes*, in *Methods in Enzymology*, D. Nejat, Editor. 2005, Academic Press. p. 431-448.

Effect of water evaporation

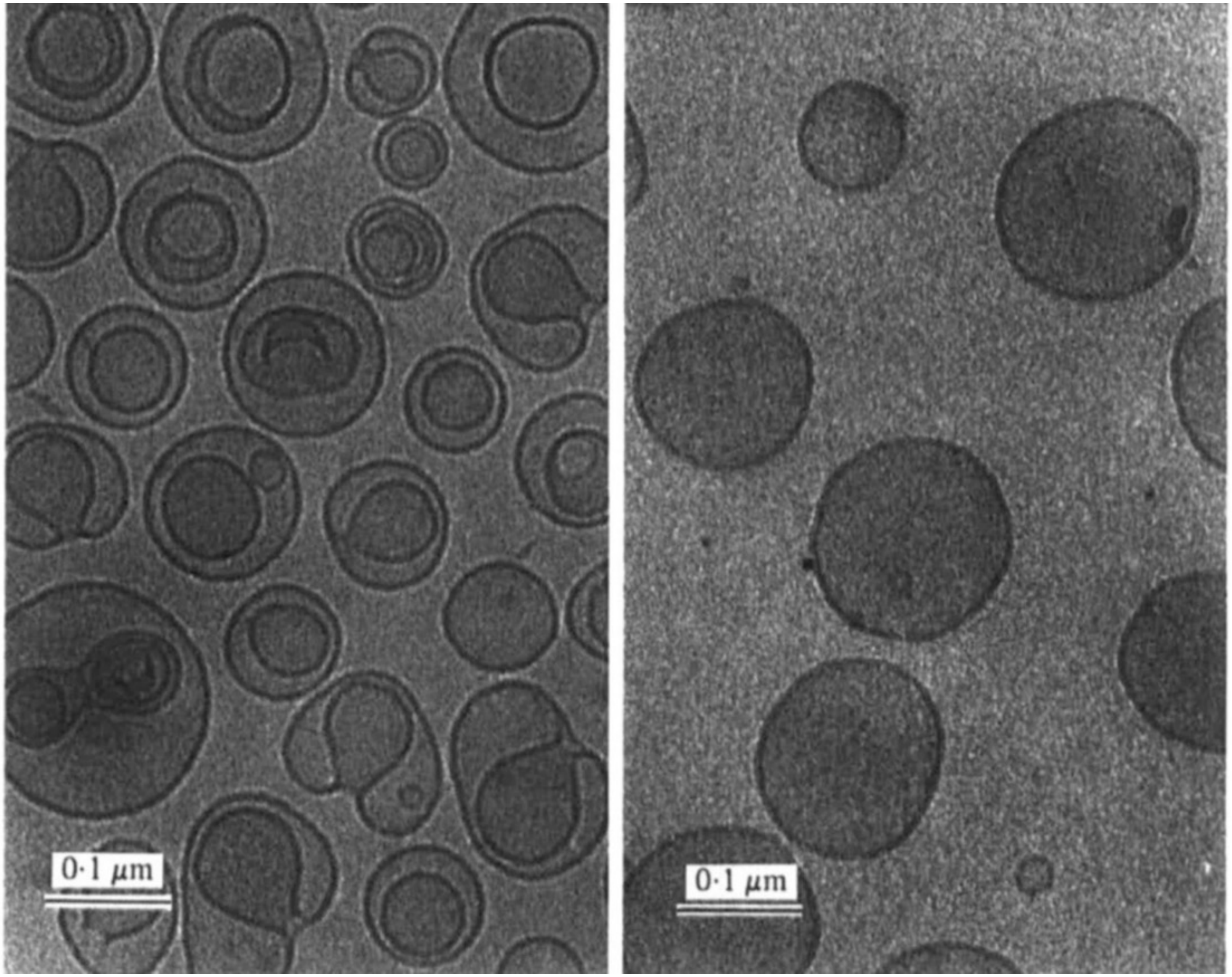

Fig. 24. Solution of lipid vesicles in 100 mM-NaCl. *(a)* The specimen has been prepared by the bare-grid method under conditions where part of the water evaporates before the thin film is vitrified. **Invagination of the vesicles and formation of concentric vesicles** reveal the osmotic effect due to the rapidly changing salt concentration in the liquid, *(b)* The same sample prepared in saturated humidity does not show osmotic effects.

Dubochet J, et al. 1988. Q Rev Biophys 21:129-228.

Automated plunge freezers

FEI

Gatan

Leica

EMS

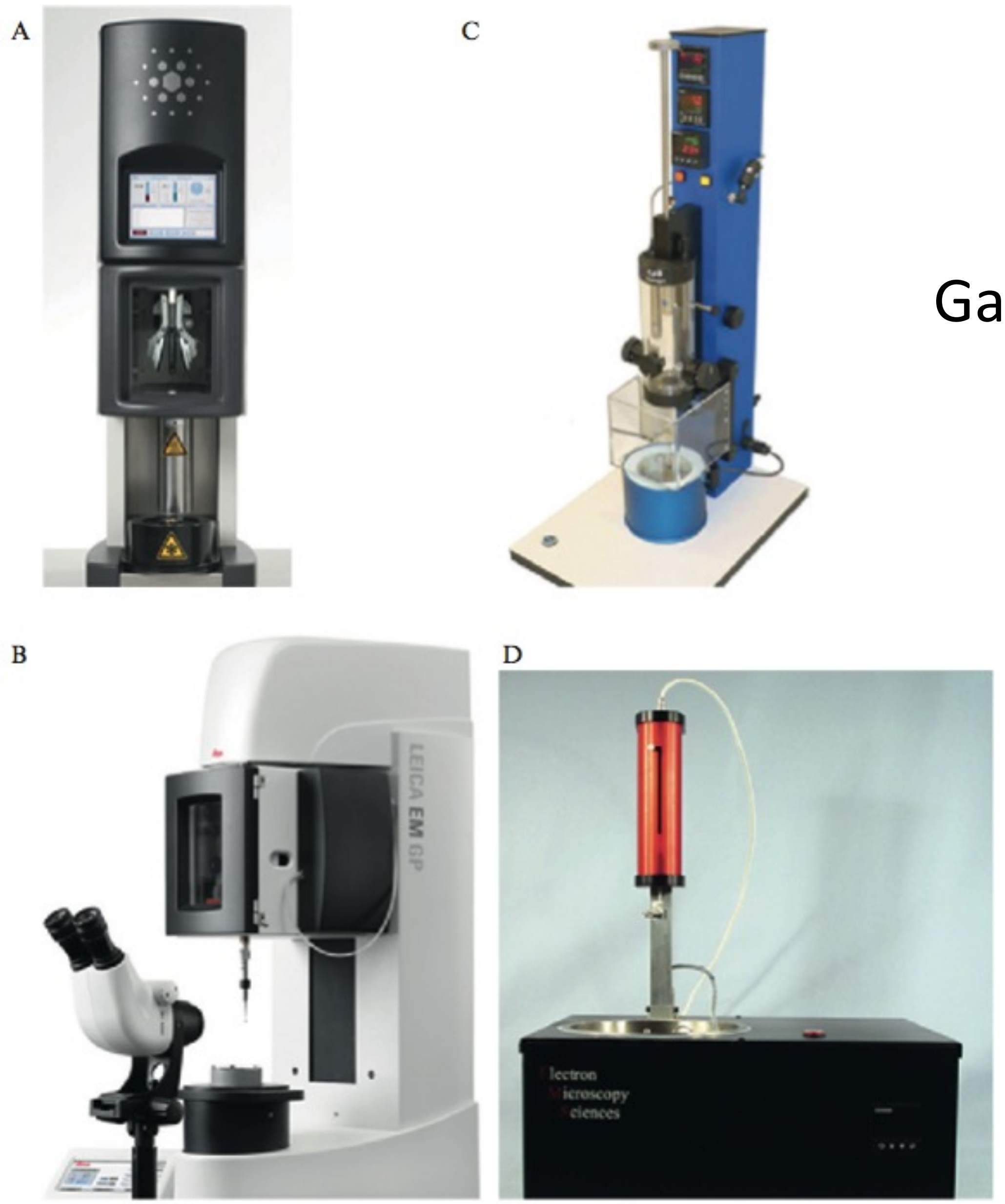

Dobro et al, MIE, 481 (2010)

Freeze samples with a Vitrobot

Automated plunge freezers

Table 1 | Deposition techniques

Deposition techniques	Devices	Methodology	Sample carrier compatibility	Stock volume	Volume per grid	Dewpoint control	Layer inspection	Time from deposition to vitrification	Grid coverage
Ultrasonic spray	Back-It-Up[83]	High-frequency droplet generation with through-grid wicking	All	0.5–1 µl	200 nl–1 µl	No	No	±130 ms	25–35%
	Shake-it-off[77]	High-frequency droplet generation with self-wicking grids	Self-wicking nanowire grids	0.5–1 µl	50 nl	No	No	<100 ms	5–10%
	De Marco group[102]	Surface acoustic waves through microfluidic device	All	0.05–5 µl	1.5–2 nl	No	No	10–1,000 ms	5–10%
Gas pressurized spray	TED (Muench group)[74]	Gas sheath around nozzle using optional high voltage to steer droplets	All	33 µl	4 µl	No	No	2–200 ms	1–5%
	Frank group[72]	Gas sheath around nozzle	All	>30 µl	9 µl	No	No	10–1,000 ms	5–10%
Electrostatic spray	Trinick group[80]	High potential difference between nozzle and grid	All	5–10 µl	1–2 µl	No	No	>1 s	5–10%
Inkjet	Spotiton[81], chameleon[85]	Droplets formed by a piezoelectric dispenser deposited onto self-wicking grids	Self-wicking nanowire grids	3–5 µl	2–16 nl	No	Yes	50–2,500 ms	10–15%
Scribing based									
Pin printing	VitroJet[89]	Dip pen deposition while maintaining dewpoint	All	0.5 µl	1 nl	Yes	Yes	1–5 s	15–25%
Capillary writing	Cryowriter[92]	Capillary deposition with controlled evaporation or reaspiration	All	15–25 nl	0.1 nl	Yes	Yes	1–3 s	10–20%

Weissenberger, et al, Nature Methods, 18, 2021, p463–471

Freeze samples with a VitroJet

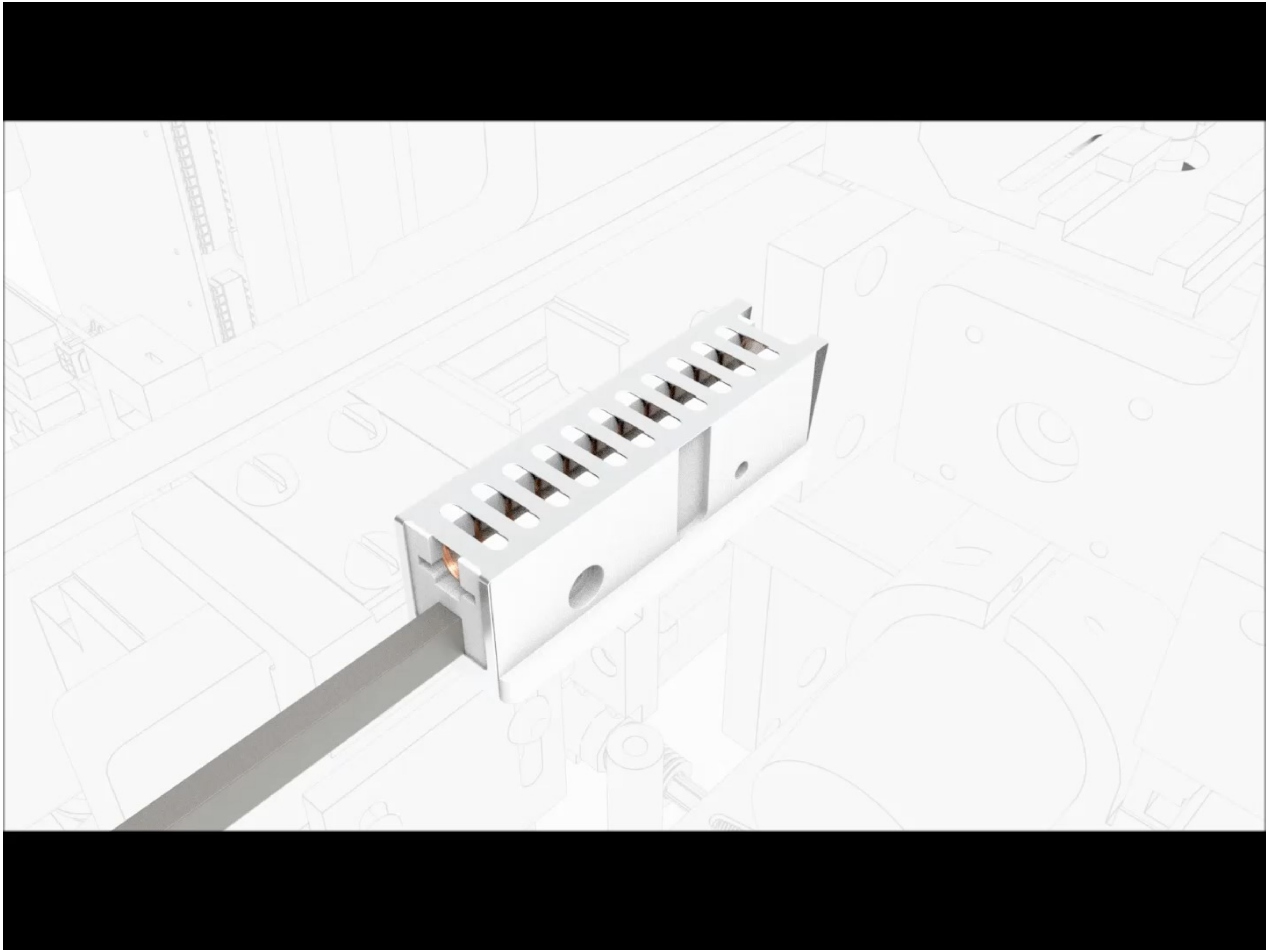

Sample screening

Experience and examples

- Good NS sample
- Bad NS sample
- Good cryo-EM samples
- Bad cryo-EM samples
- Weird ice
- Denatured-particle “skin”
- Tips to reduce ice contaminations

Good NS examples: continuous carbon grids

550x

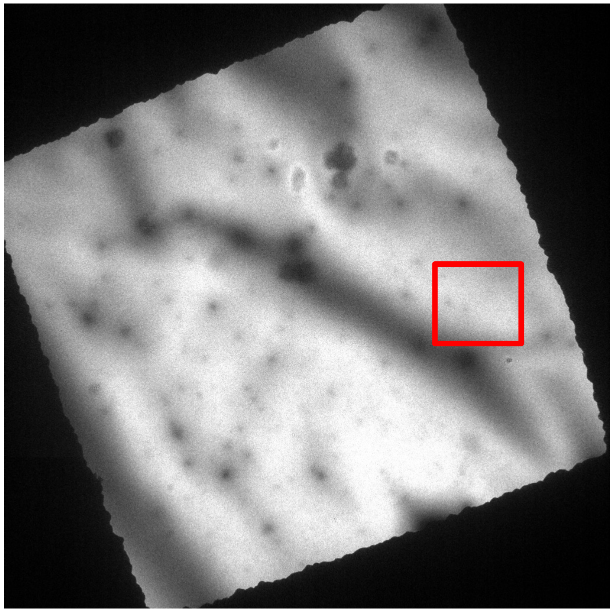

8500x

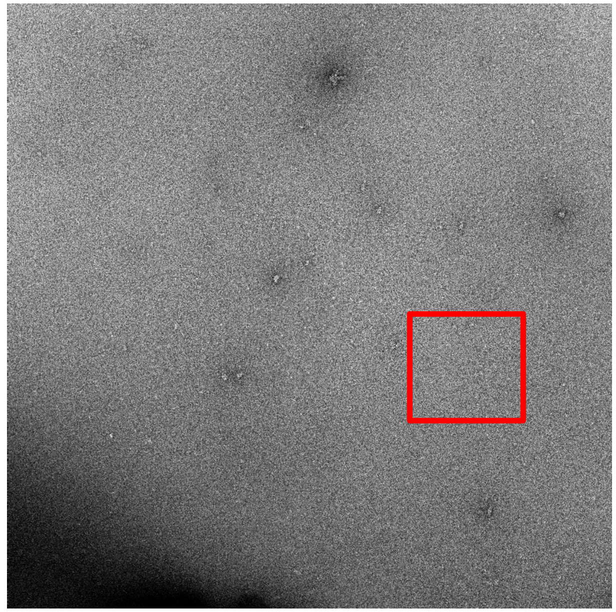

120kx

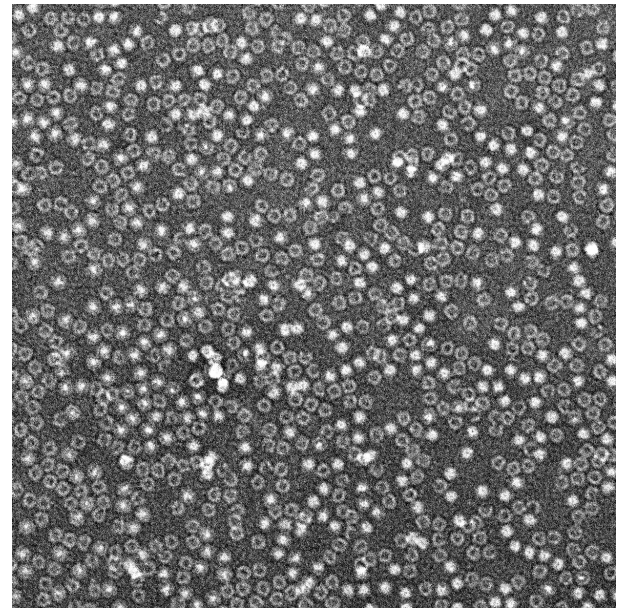

100x dilution

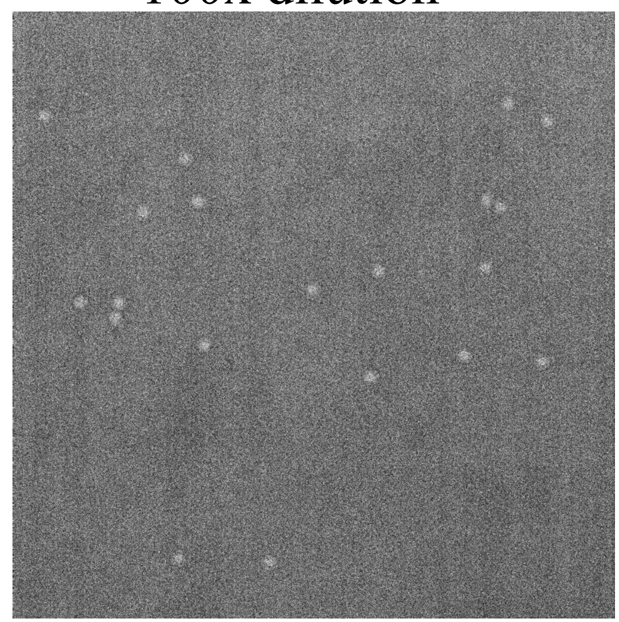

- 400 mesh continuous carbon (recommended)
- 20 mA, 20s glow discharge
- 60s 6uL sample + blot,
  60s Nano-W + blot,
  60s Nano-W + blot to dry

Bad examples

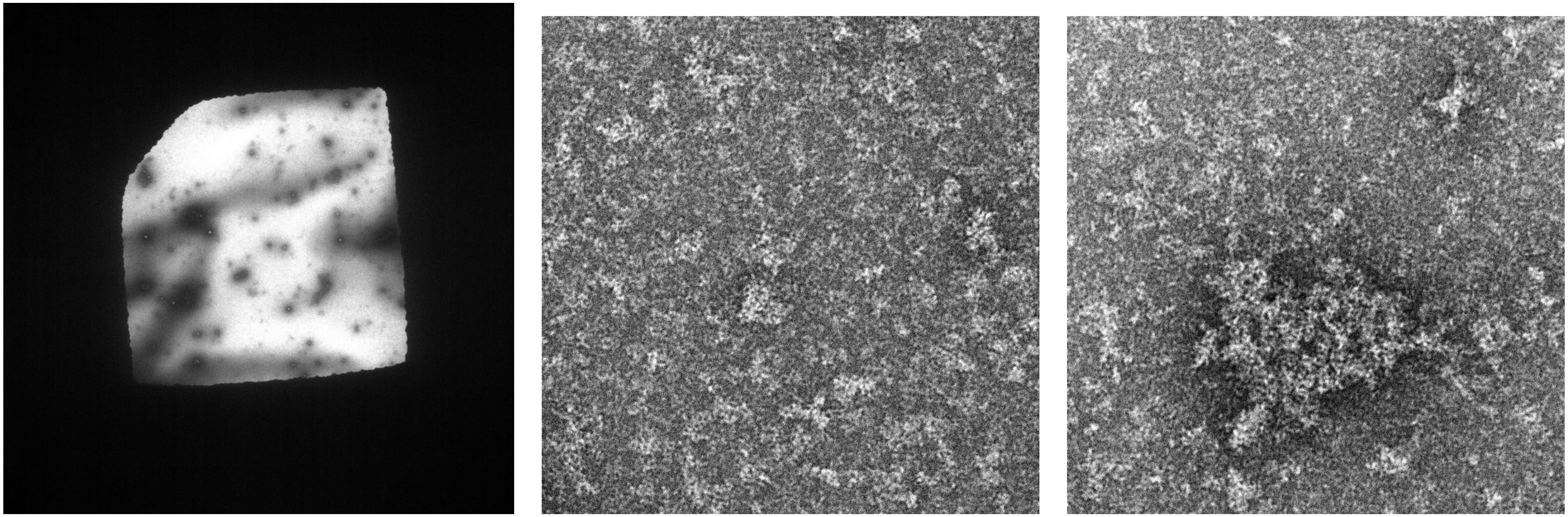

- Heterogenous particles
- Aggregates

Good examples: holey carbon grids

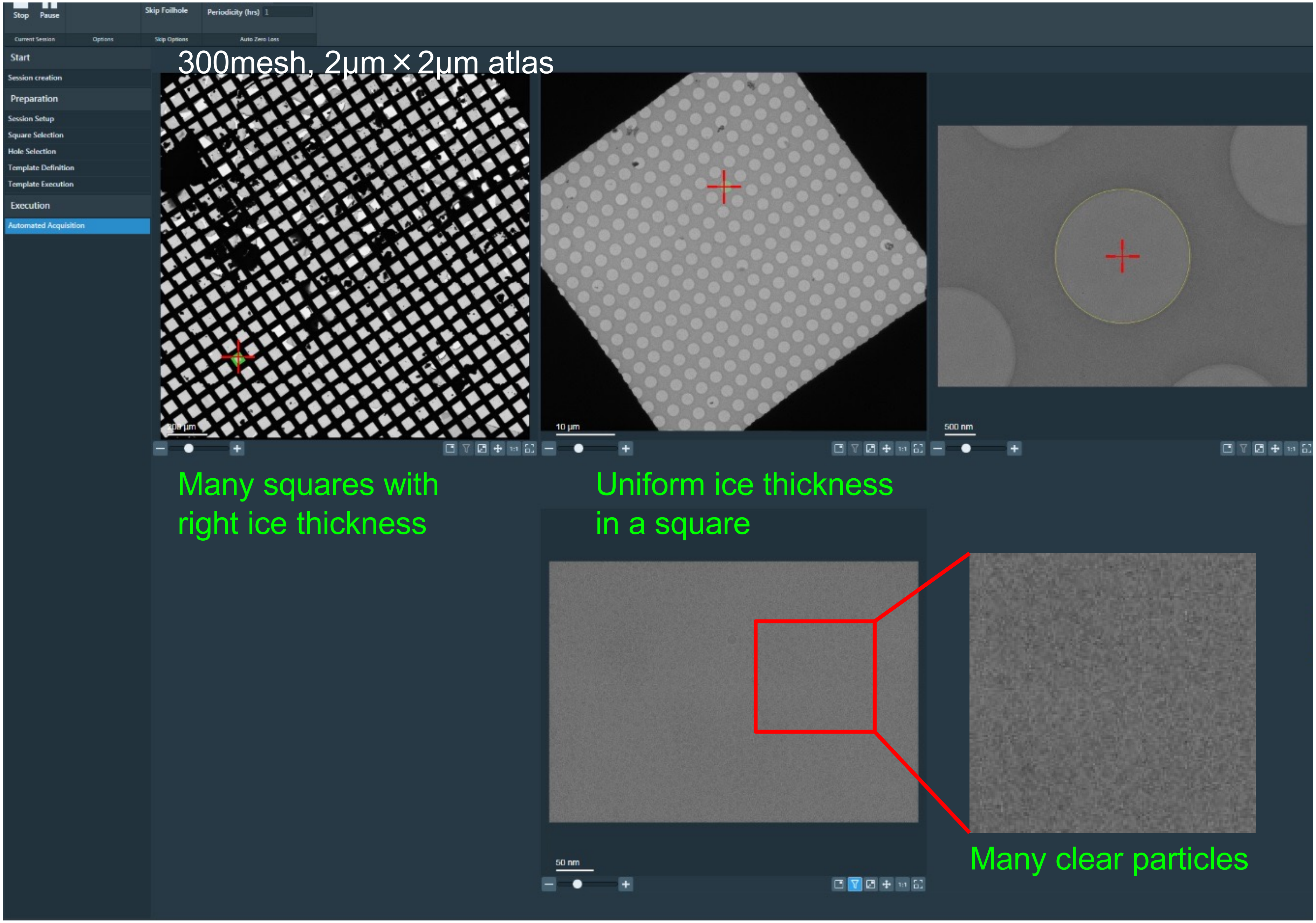

Good examples: holey gold grids

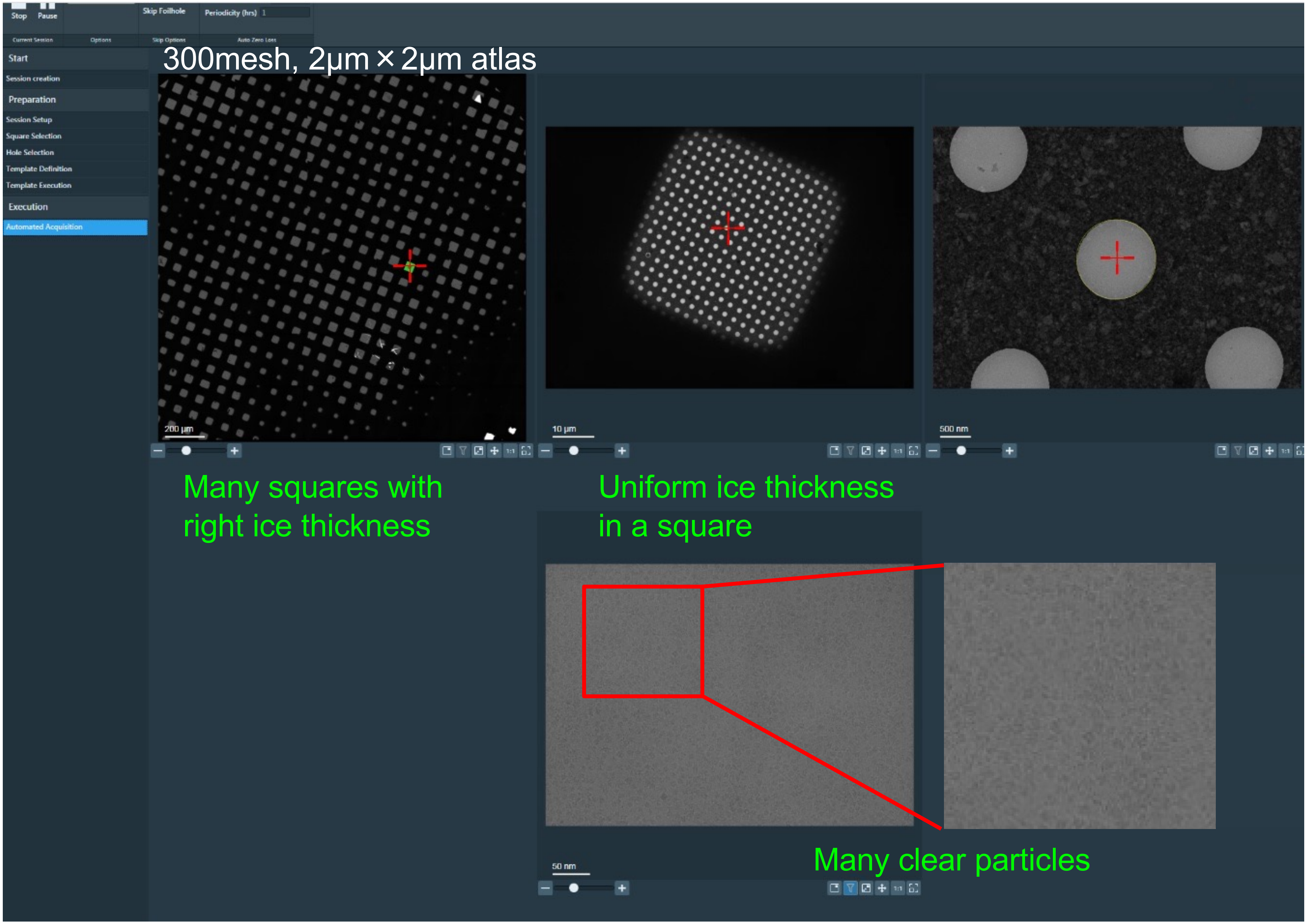

2umx2um atlas

Bad examples

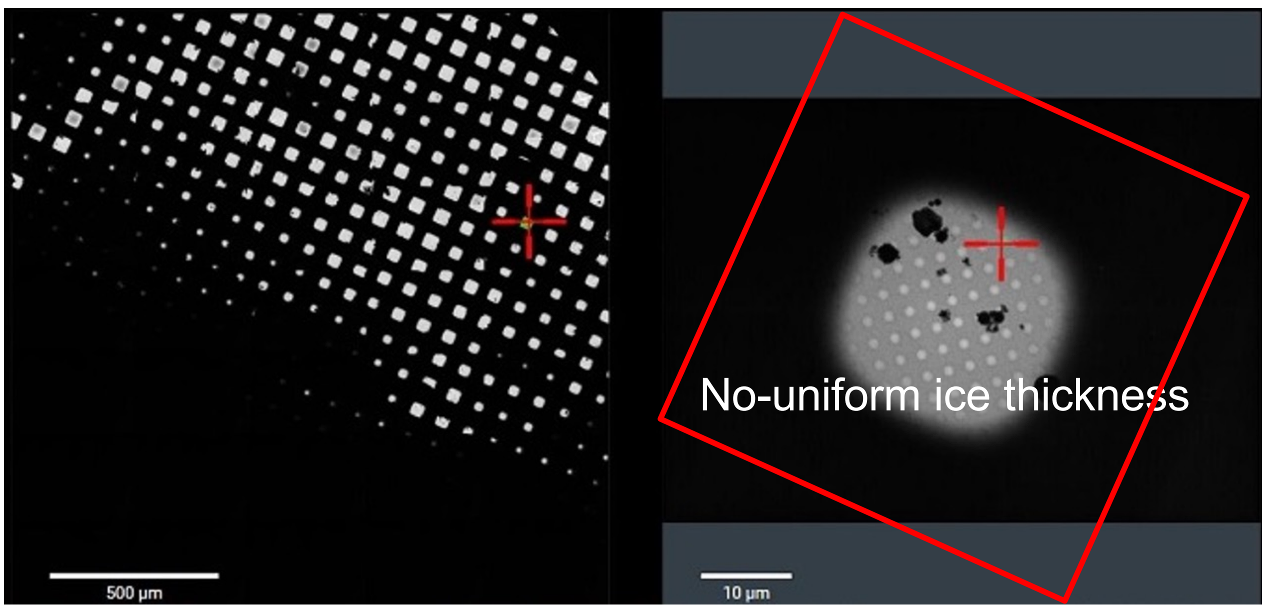

2umx2um atlas

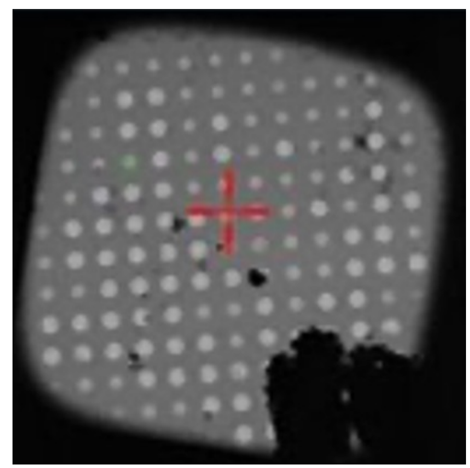

Bad examples

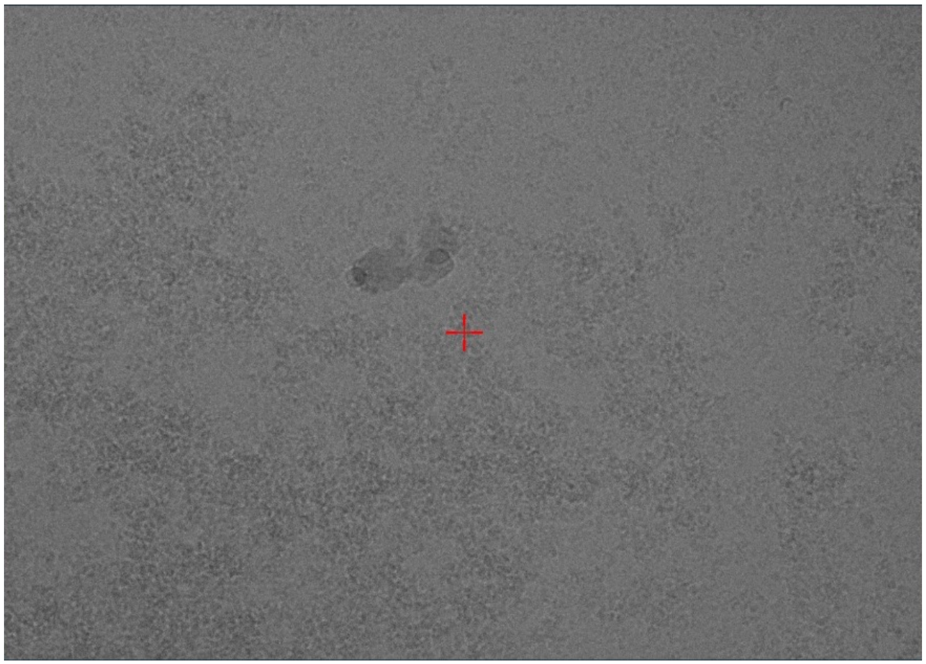

Protein aggregates

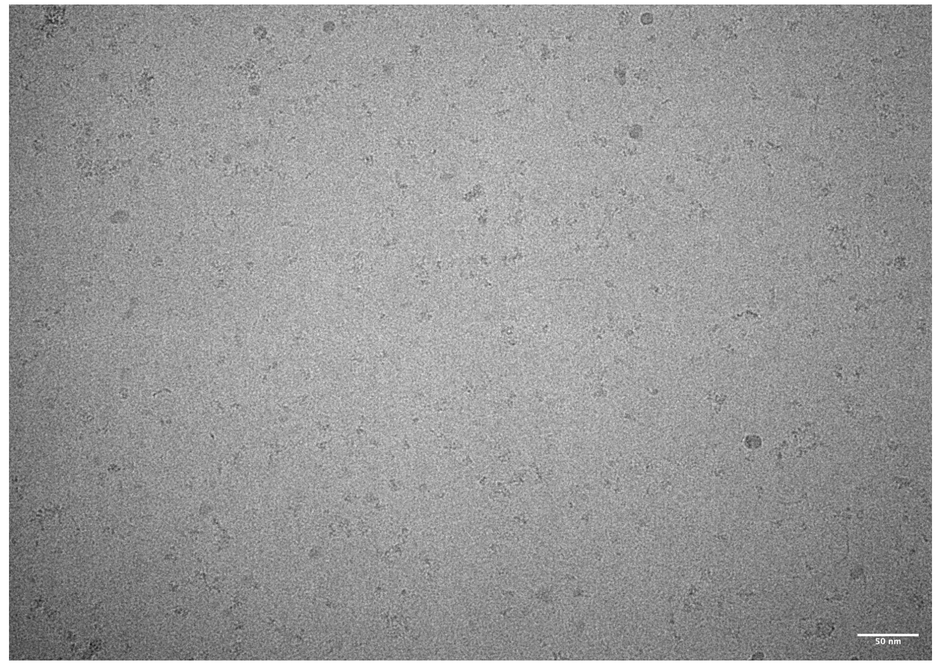

Low particle density

Bad examples

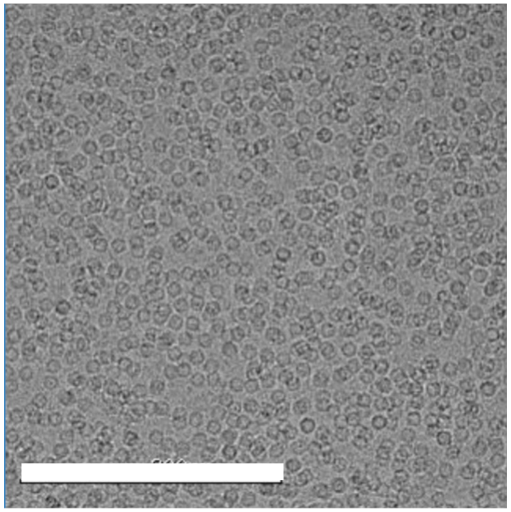

(a) Too dense

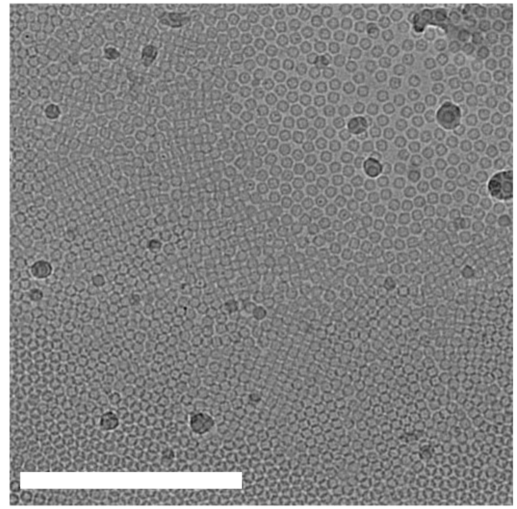

(b) Partially too dense

White bars are 200 nm in length.

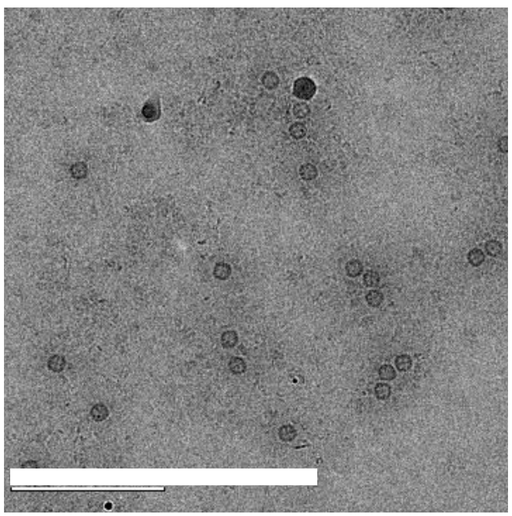

(c) Too sparse

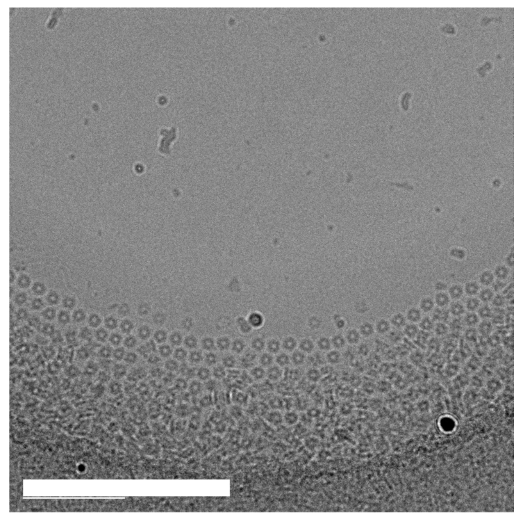

(d) Ice thickness-dependent concentration & orientation distribution

Wang, L. and C.M. Zimanyi, Acta Crystallogr F Struct Biol Commun, 2024

“Leopard ice”, "turtle-ice”, “alligator ice”, "dried mud"

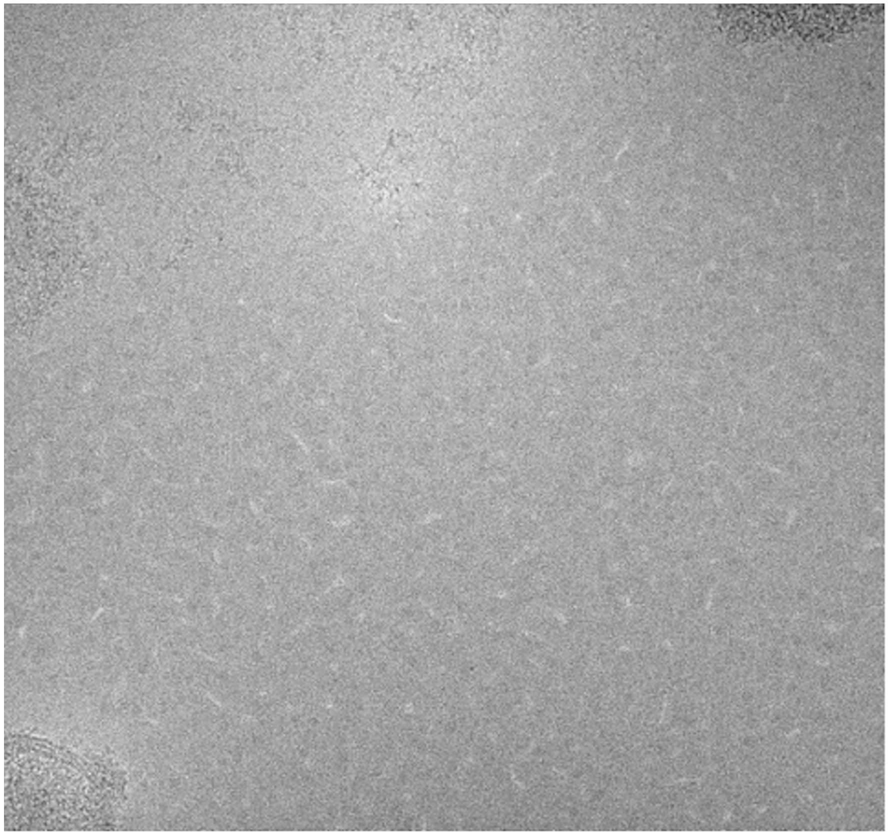

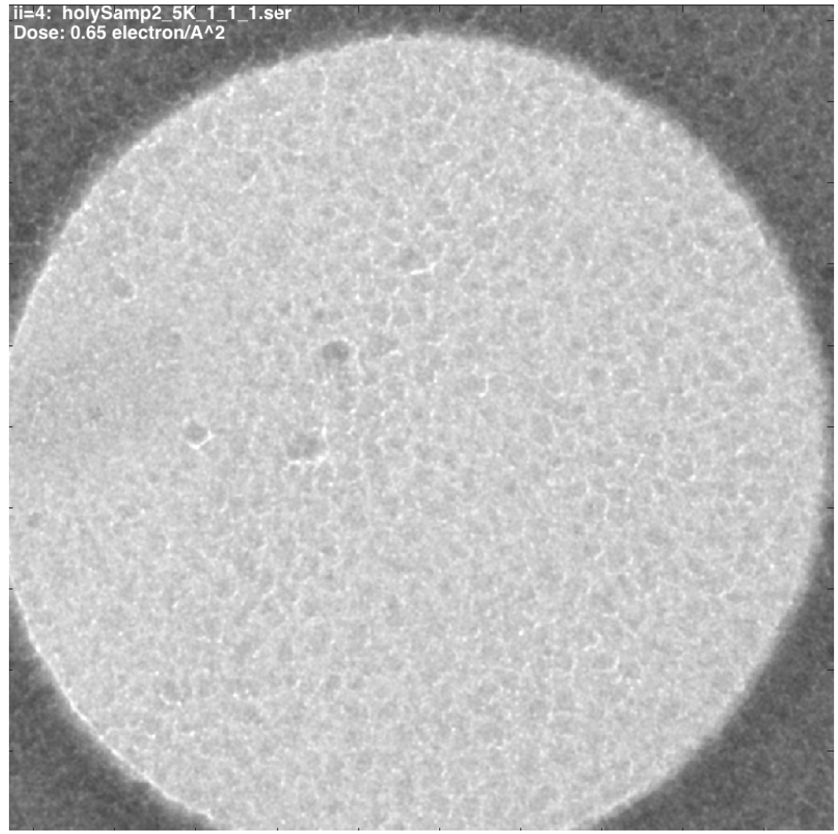

? Ice form

More than one source of the problem and usually not reproducible

- Transfer of the cryoholder is likely the most common one
- Not having filled the nitrogen high enough in the dewar
- Not cooling the ethane long enough
- Sample in the EM is not cold enough. Water sublimates and recrystallizes nearby.

Courtesy: Yutong Song

Features observed in cryo-samples

Denatured-particle “skin”: some types of protein can rapidly form a monolayer “skin” of denatured protein at the air-water interface,

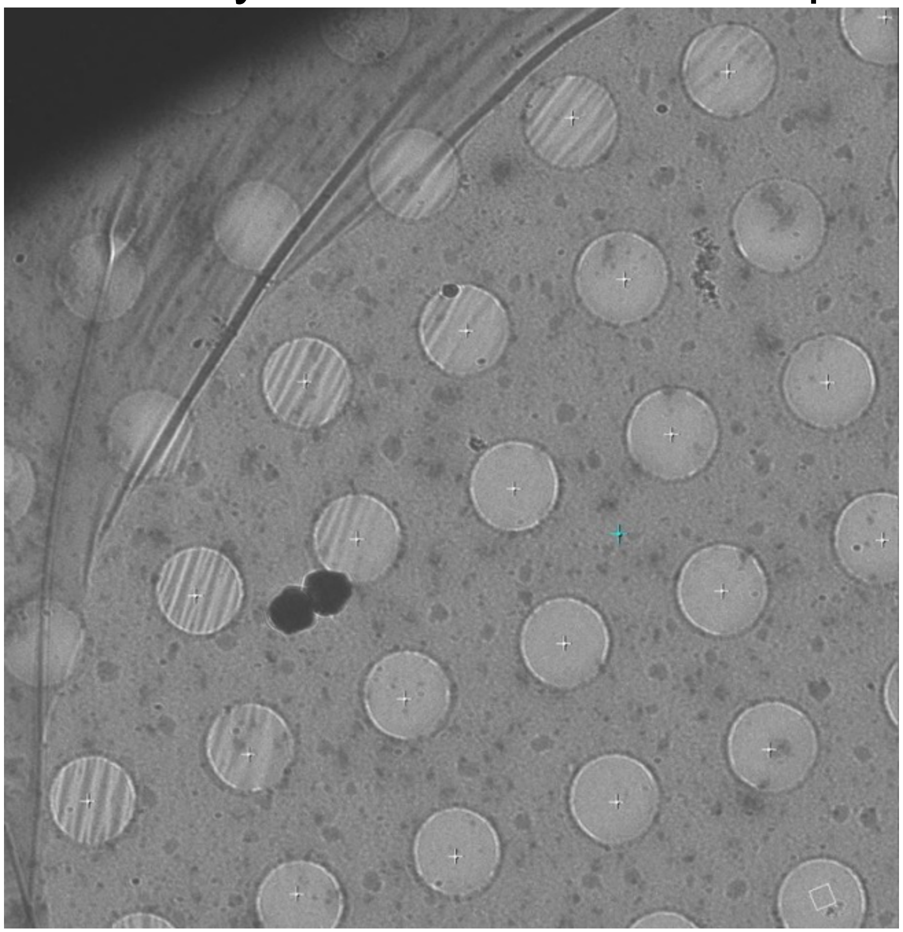

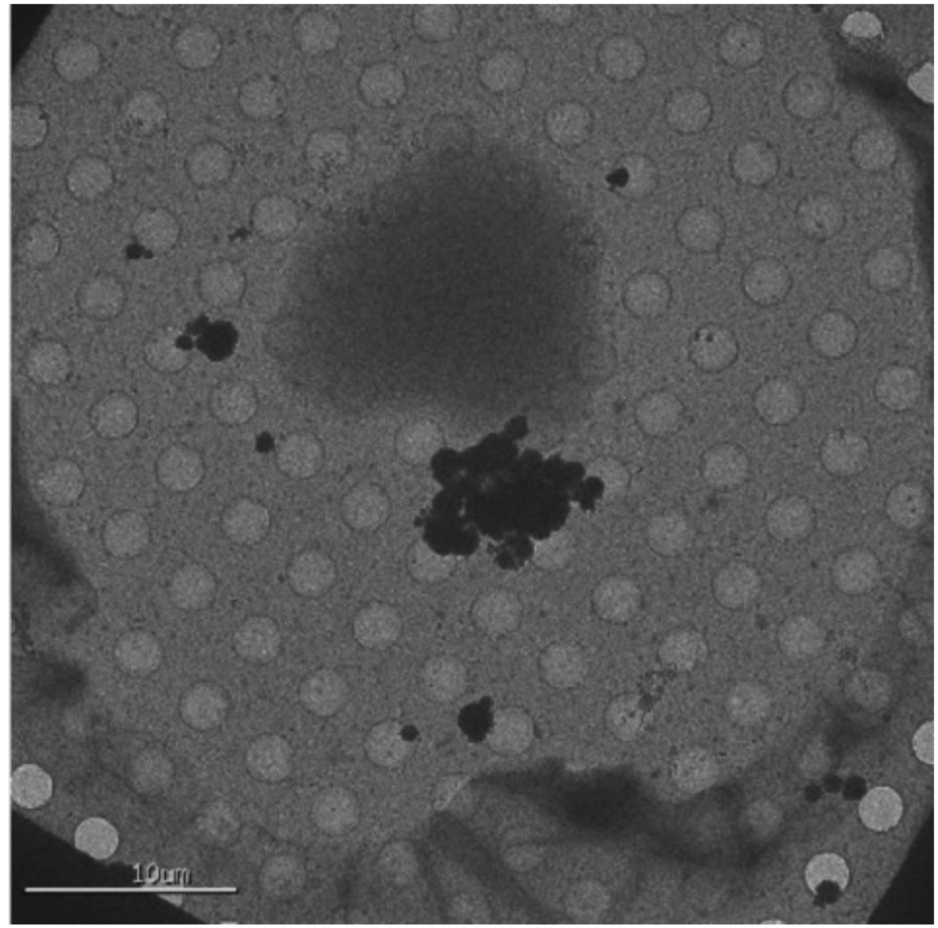

Han, BG et al. J Struct Biol. 2016 August ; 195(2): 238–244. doi:10.1016/j.jsb.2016.06.009.

Sample preparation tips

- Really plan your experiment!
- Get everything ready before pouring LN2
  e.g. grid box, storage tube, 1L dewar, tweezers (sample number+1), grids, plunger (tested), filter paper, samples, pipette, pipette tips, timer, long tweezer, screw driver, etc
- Check ethane level to ensure immersion of the grid
- Cover flask containing grid box after topping off the flask, and don't cover it after starting freezing samples.
- Grids: 400 mesh grids for NS
  300 mesh grids for cryo-samples
- Glow discharge:
  20-30mA, 20 s for carbon / 120 s for gold;
  10 mA, 5s for ultrathin carbon coated holey grids

Advanced topics

- Ethane and propane mixture
- Glycerol in sample
- Air-water interface
- Ice thickness measurement

Ethane and Propane mixture

- **Do not solidify** when at the temperature of liquid nitrogen
  63% propane and 37% Ethane: -196 ^{o}C melting temperature

	Melting Point (^{o}C)	Boiling Point (^{o}C)	Heat of vaporization (kJ/kg)	Heat capacity (kJ/(kg·K)	Heat to boil (kJ/kg)	Heat to evaporate (kJ/kg)	Liquid density (kg/m3)
Nitrogen	-210	-196	6	0.9-1.6	13-22	19-28	809
Ethane	-183	-89	489	2.3-3.5	216-329	705-818	546
Propane	-188	-42	428	1.63	238	666	580
Water	0	100	2257	4.185	418.5	2675.5	1000

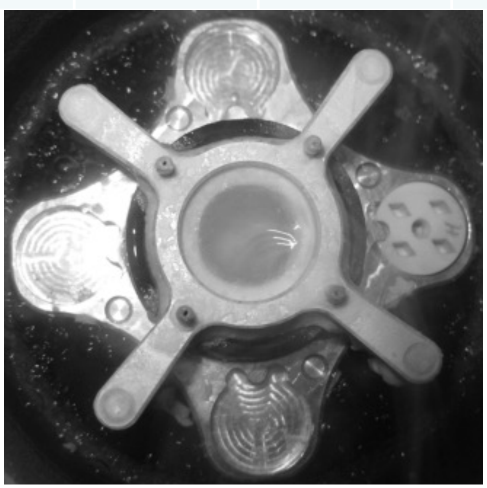

- Ethane cooled directly with LN2: solidify completely
- Ethane insulated from LN2: solid ethane melts and at unknown temperature

Cheng, D., Mitchell, D., Shieh, D.-B., & Braet, F. (2012). Practical Considerations in the Successful Preparation of Specimens for Thin-Film Cryo-Transmission Electron Microscopy.

Ethane and Propane mixture

- **Do not solidify** when at the temperature of liquid nitrogen
  63% propane and 37% Ethane: -196 ^{o}C melting temperature

Thermally isolated cup

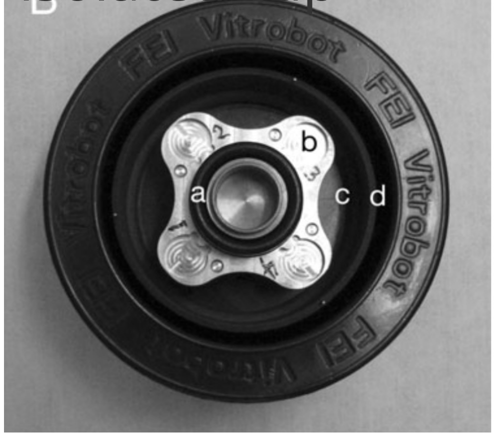

Direct contact of the cup with LN2

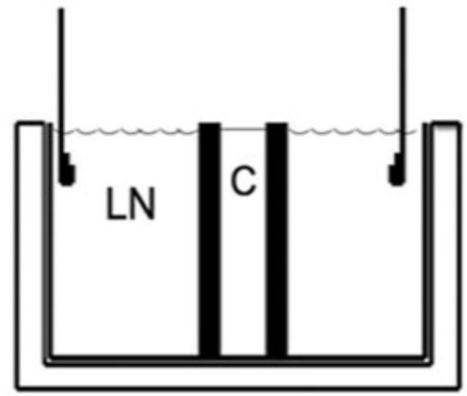

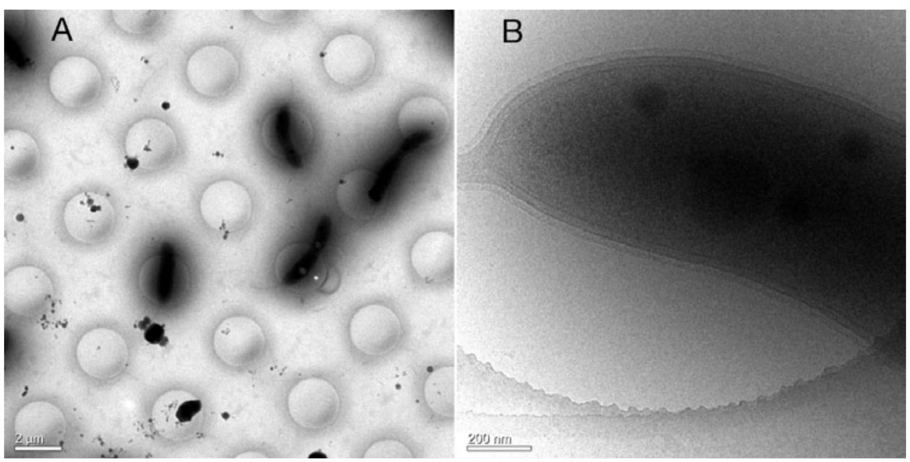

Freezing with Pr-Et using Vitrobot. bacterium embedded in amorphous ice.

Tivol, W. F., Briegel, A., & Jensen, G. J. (2008). An Improved Cryogen for Plunge Freezing. Microscopy and Microanalysis, 14(5), 375-379. doi:10.1017/S1431927608080781

Glycerol?

- Why is it strongly discouraged by cryo-EM community?
  * Decrease image contrast
  * Increase beam-induced motion
  * Increase sensitivity to radiation damage (”bubbling”)

- Recent investigation:
  - With up to 20% glycerol, high resolution structure can be determined: 2.3 Å apoferritin, 3.3 Å aldolase
  - Some disadvantages exist

Similar beam-induced motion

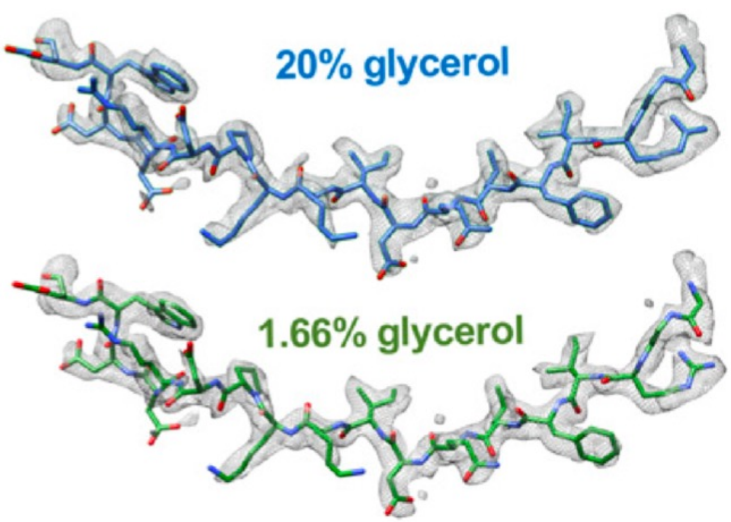

Residues 78-94 of PDB 6V21 fit into density

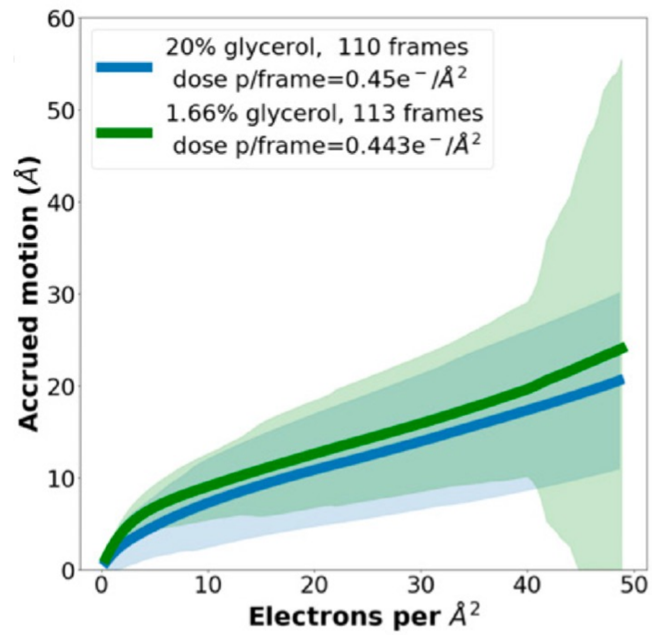

bioRxiv preprint doi: https://doi.org/10.1101/2021.09.10.459874

Glycerol: disadvantages

- Longer blotting time: nearly two-fold for the 20% glycerol sample

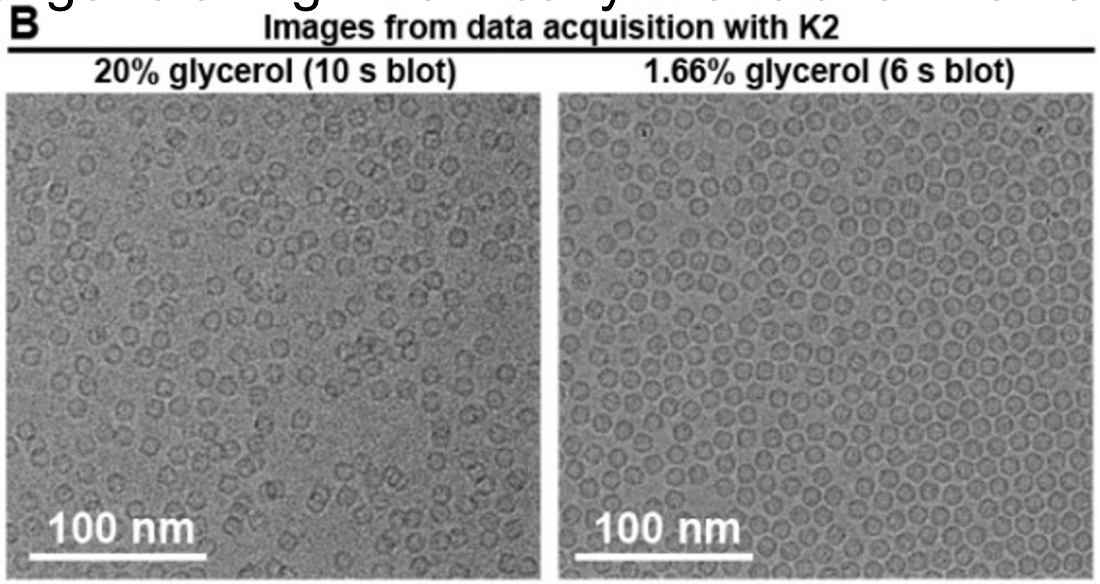

- Thicker ice and larger variation even with longer blotting time

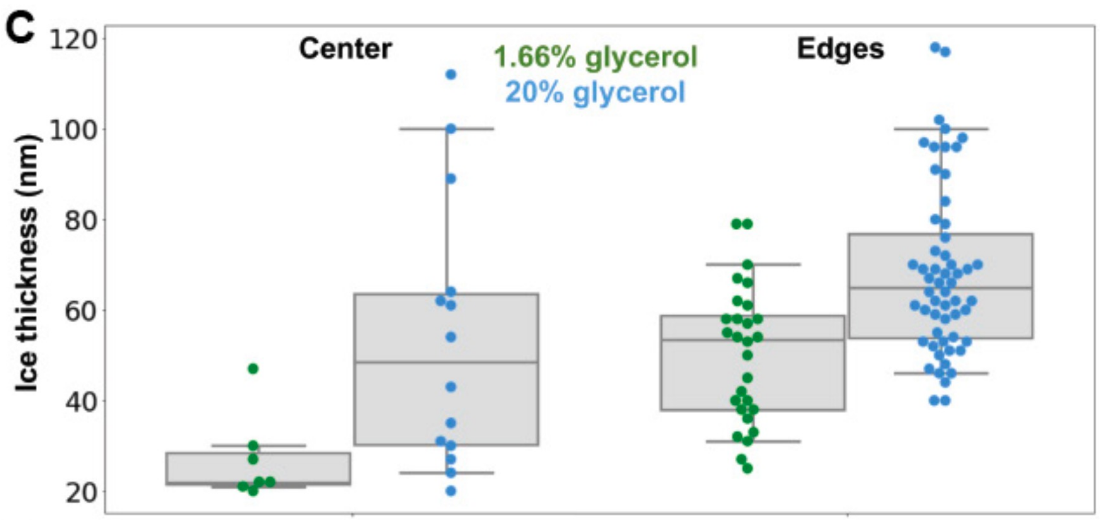

bioRxiv preprint doi: https://doi.org/10.1101/2021.09.10.459874

Glycerol: disadvantages

- Complicated data processing and larger B-factor: apoferritin @200keV

1.66% glycerol

Map sharpening B-factor: -19 Å^2

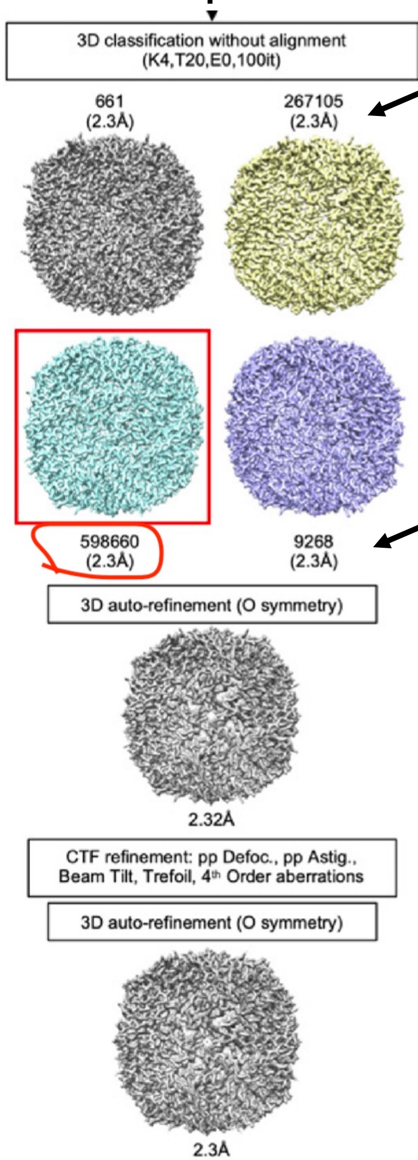

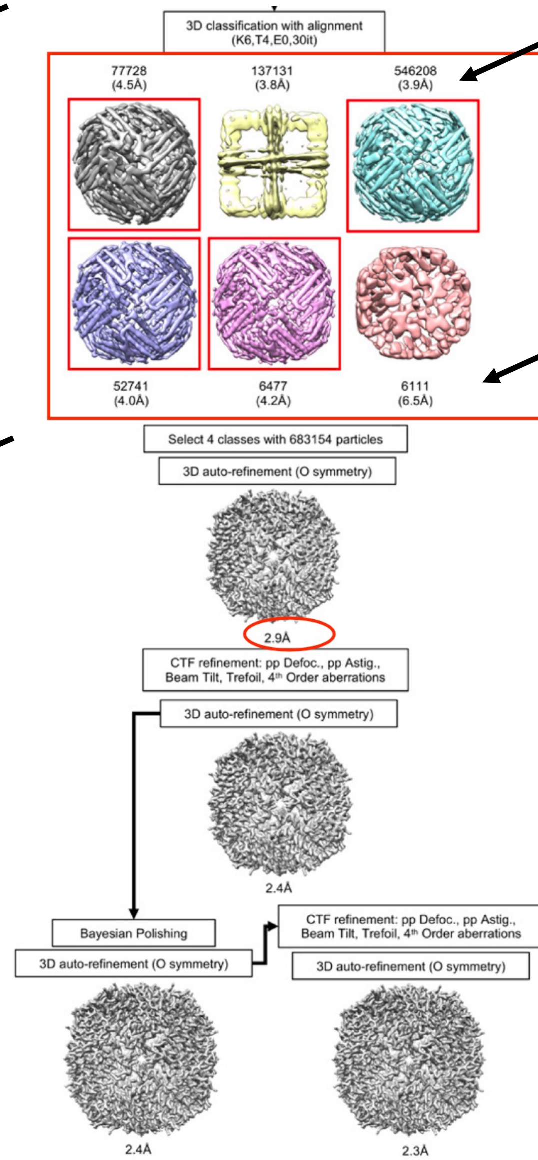

20% glycerol

Map sharpening B-factor: -36 Å^2

bioRxiv preprint doi: https://doi.org/10.1101/2021.09.10.459874

Air-water interface

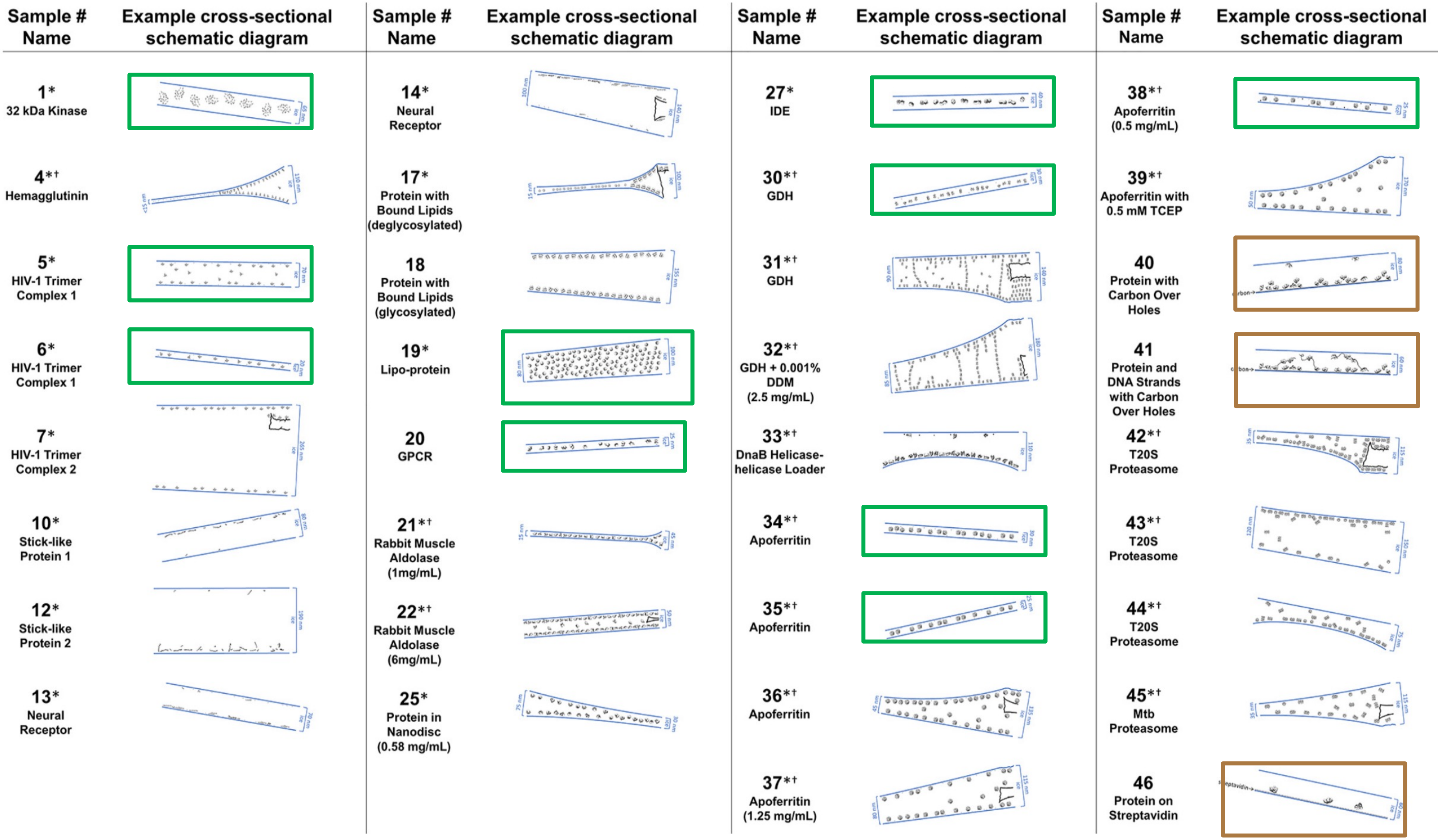

Noble et al. eLife 2018;7:e34257. DOI: https://doi.org/10.7554/eLife.34257

Method to measure ice thickness

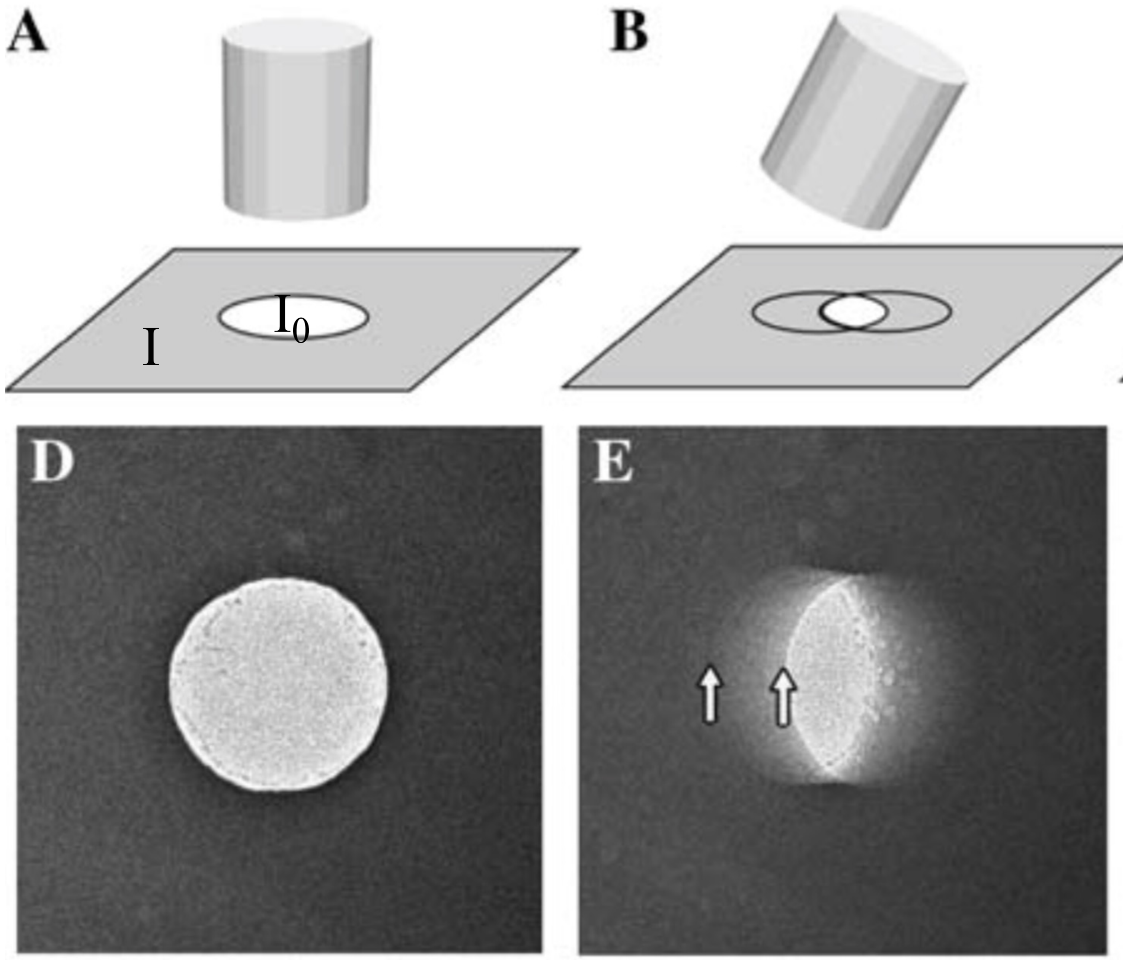

$t = k * \ln(I_0/I)$

t: ice thickness (nm)
k: constant (nm)
I_0: image intensity of a hole
I: image intensity

A. Cheng et al. / Journal of Structural Biology 154 (2006) 303–311

Method to measure ice thickness

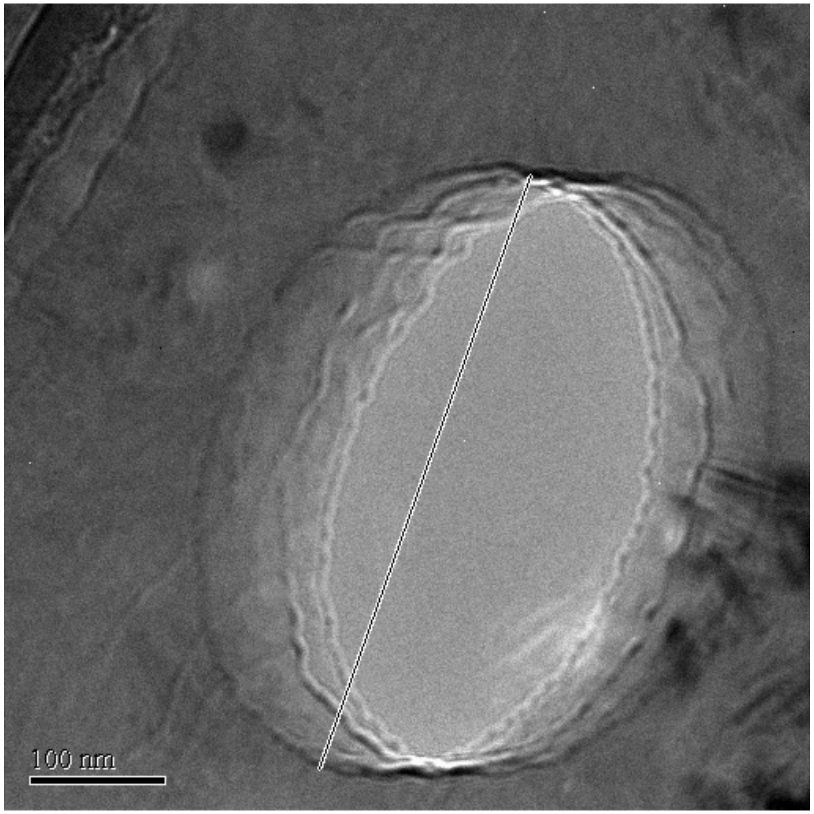

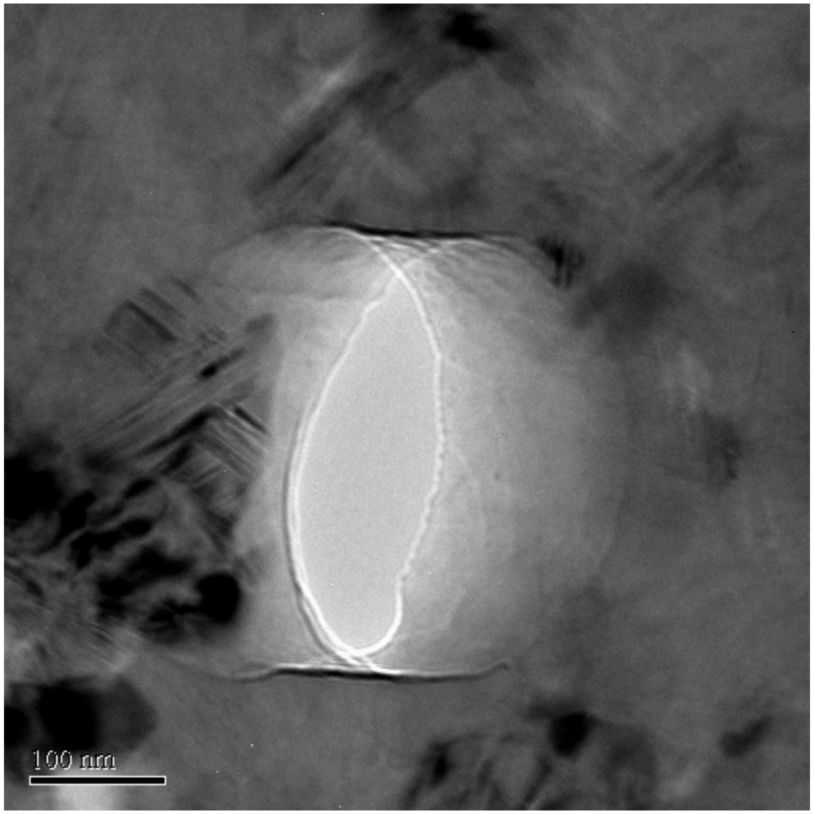

Note: important to use really thick ice

Measure ice thickness with tomography

Apparent mean free path for inelastic scattering $d = \Lambda \ln \frac{I}{I_{zlp}}$ with and without GIF

Microscope	Voltage (keV)	Slit Width (eV)	Apparent MFP for inelastic scattering (nm)	Method
Titan Krios	300	15	395 +/– 11	Tomography
Titan Krios	300	20	435 +/– 30	Compare with 15 eV

ALS coefficients $d = \lambda \ln \frac{I_0}{I}$ with and without samp

Microscope	Voltage (keV)	Obj. Aperture diameter (μm)	Lambda (nm)	Method
Titan Krios 20 eV slit	300	100	322	compare with EF determination
Titan Krios (no EF)	300	100	3,329	Aldolase thickness
Titan Krios (no EF)	300	none	78,788 *	Aldolase thickness
Tecnai F20	200	100	392	Tomography
Tecnai F20	200	70	302	Compare with 100 μm
Tecnai T12	120	100	319	Tomography
Tecnai T12	120	70	247	Compare with 100 μm

W. Rice, et al. J Struct Biol. 2018 October ; 204(1): 38–44

Ice thickness measurement at LBMS

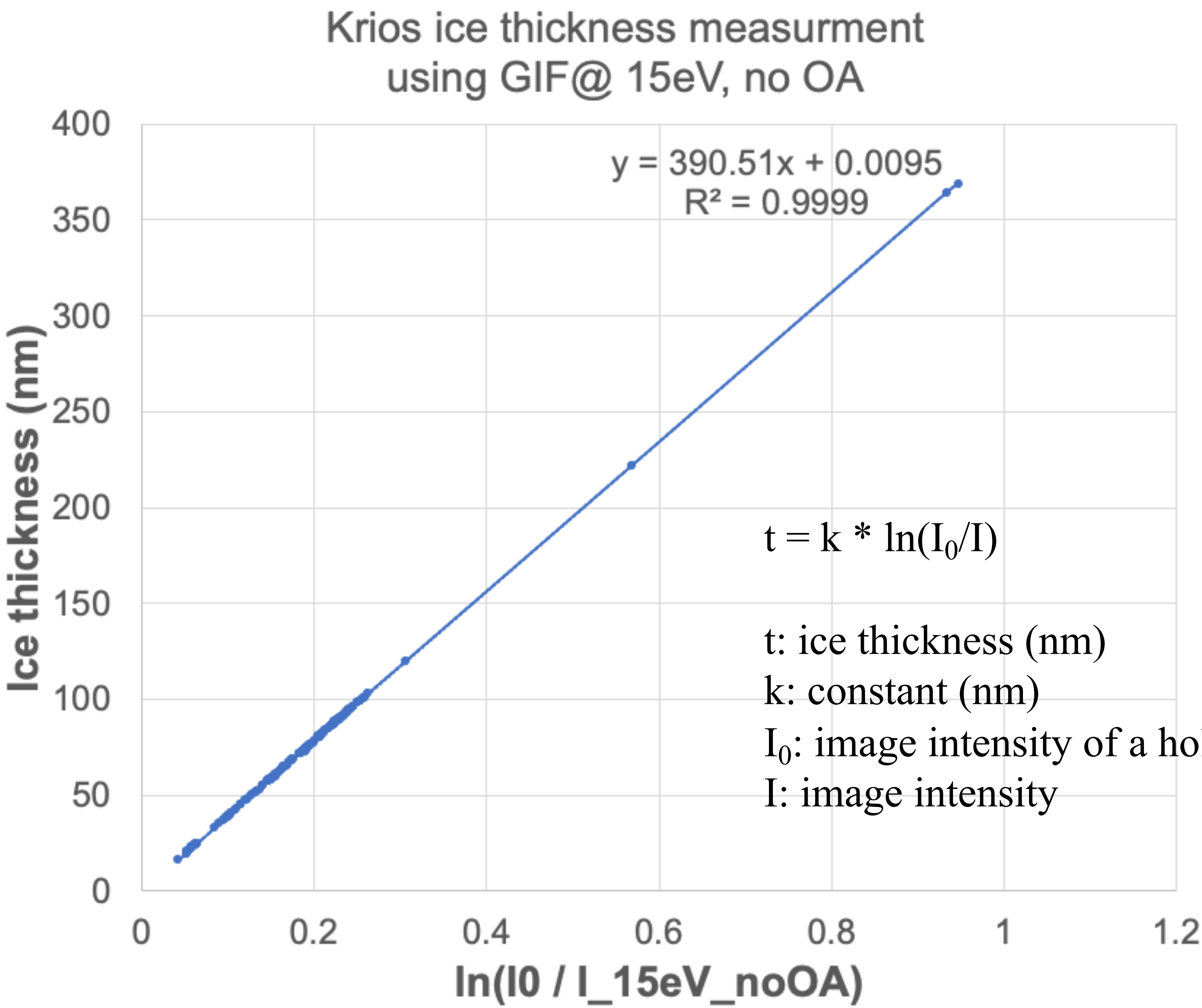

$t = k * \ln(I_0/I)$

t: ice thickness (nm)

k: constant (nm)

I_0: image intensity of a hole

I: image intensity

Thanks!

Cryo-EM sample screening

- Keep sample at cryogenic temperature
- Reduce ice contamination
- Reduce radiation damage
- Measure ice thickness

Krios EM: autogrid and autoloader

Krios G3i up to 5 days with no observable contamination accumulation

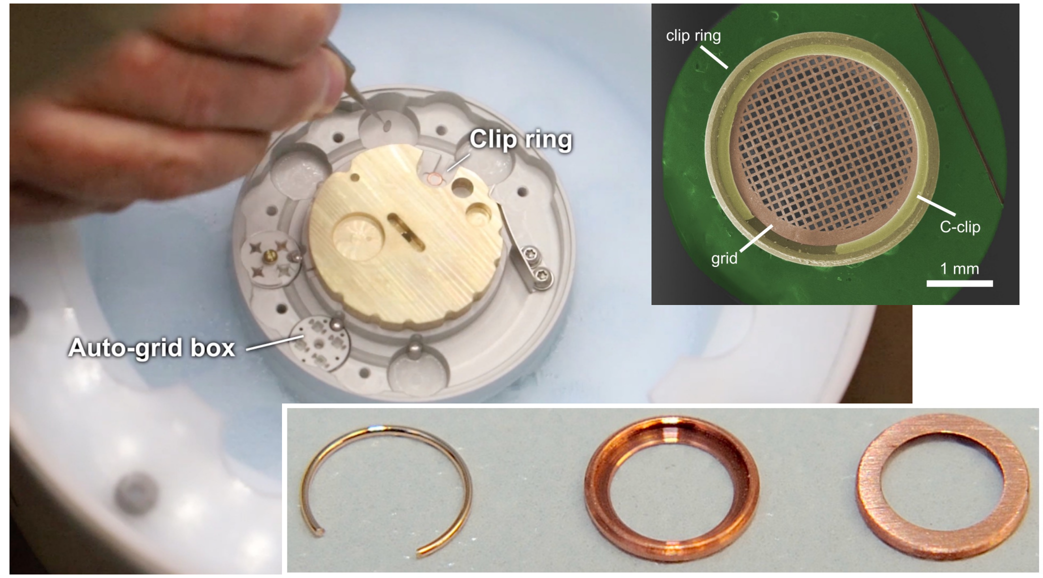

https://cryoem101.org/chapter-3/
https://vimeo.com/492720742

Autogrids for Krios

Autogrid

C-clip ring

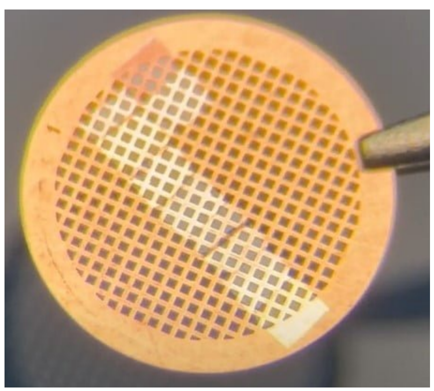

C-clip ring

Side-entry EMs: cryo-holder and anti-contaminator

Tecnai TF20

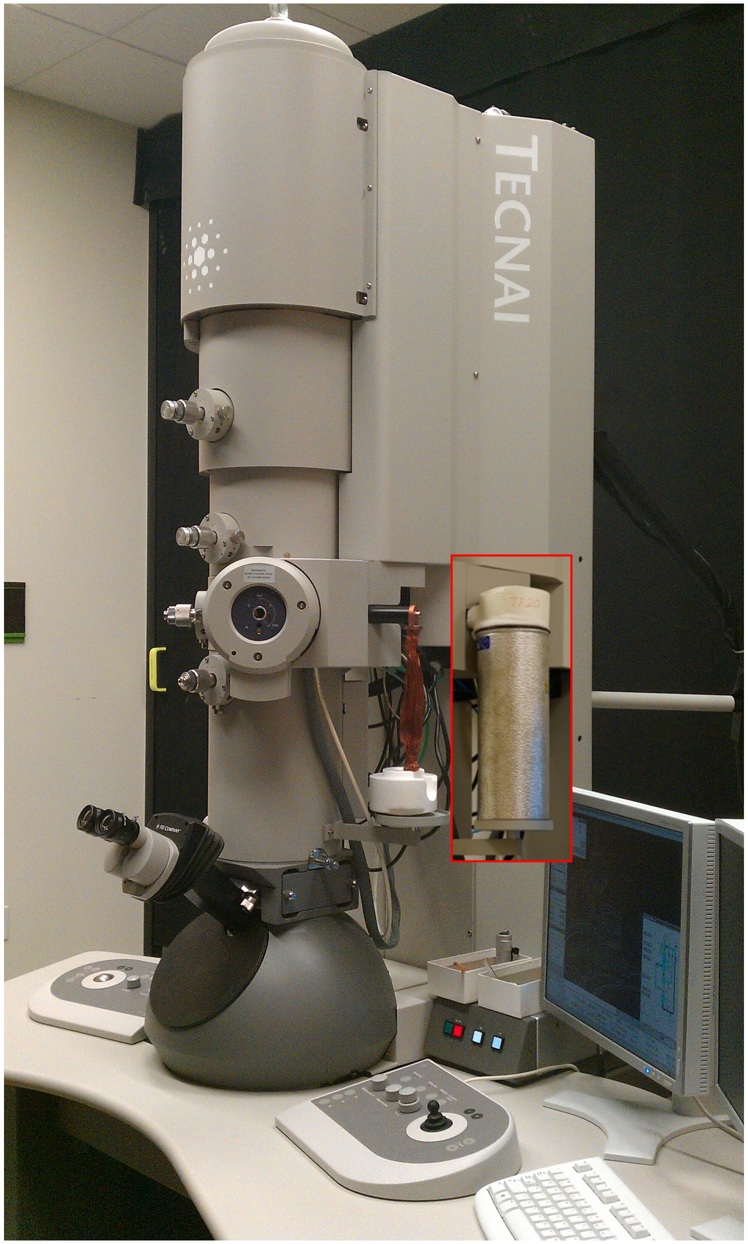

Cryo-box

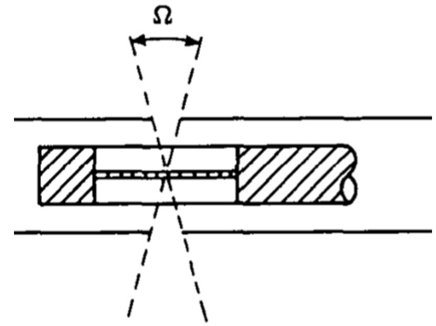

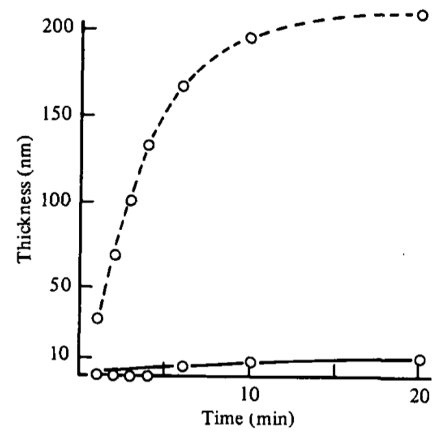

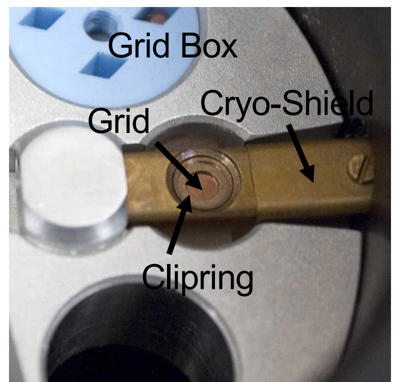

Low dose to reduce radiation damage

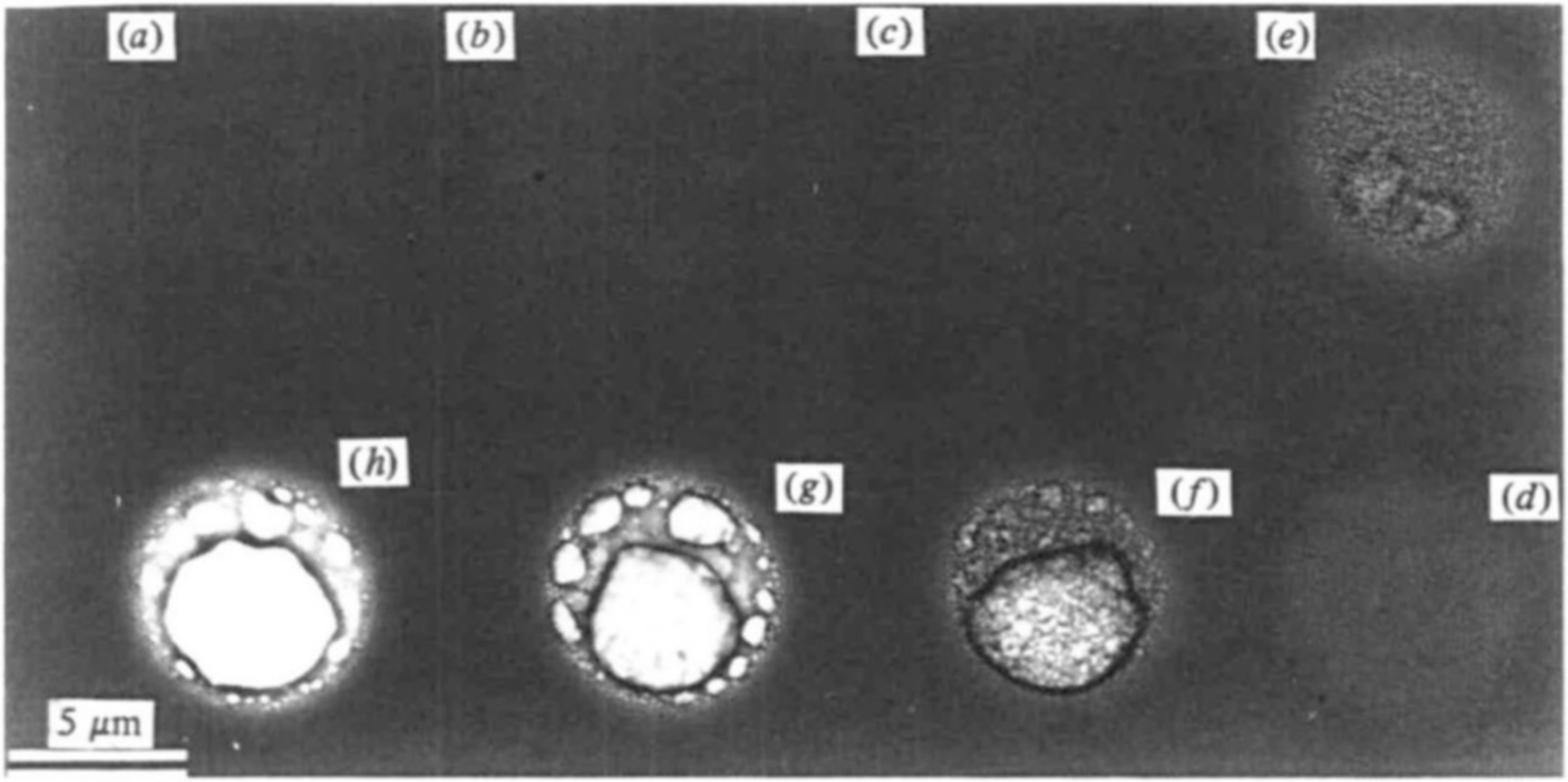

Fig. 37. Bubbling on a carbon-coated formvar film c. 10 nm thick, covered with a layer of condensed vitreous water. Fields (a)-(h) correspond to irradiations by 5, 20, 40, 80, 120, 240, 340 and 450 ke/nm2 respectively. The total thickness of the specimen is 160 nm.

Low dose to reduce radiation damage

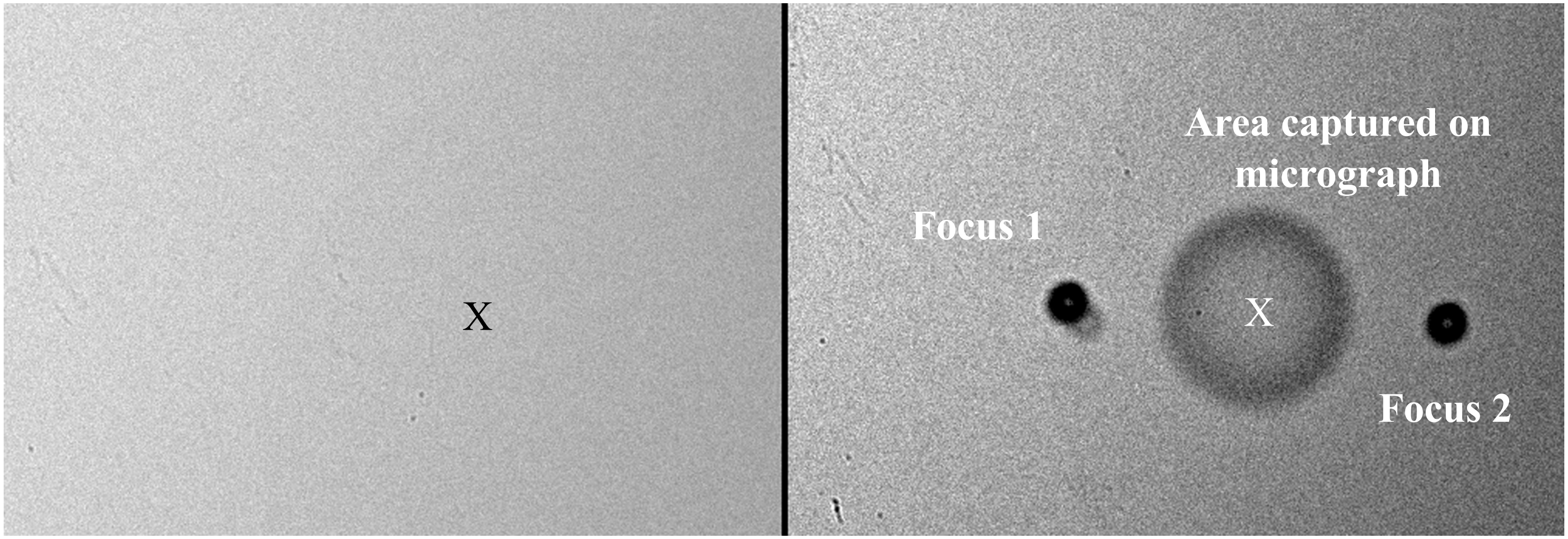

Appearance of trehalose dried down on a carbon film (left). The sugar allows to demonstrate how "low-dose" microscopy is done (right). Let X be the area of interest (for instance a crystal or virus/single particle). Prior to taking a picture some parameters such as "defocus" and "astigmatism" need to be adjusted. To avoid destruction of the specimen, any adjustments are made on small areas (Focus 1 and 2) located adjacent to the area that will be photographed. In the example, the trehalose burned as it was exposed at high magnification (220kx, Focus 1 and 2). Similarly, by exposing the area to be captured for about 30 seconds at 52,000 fold magnification.

Electron optics of Low-Dose imaging

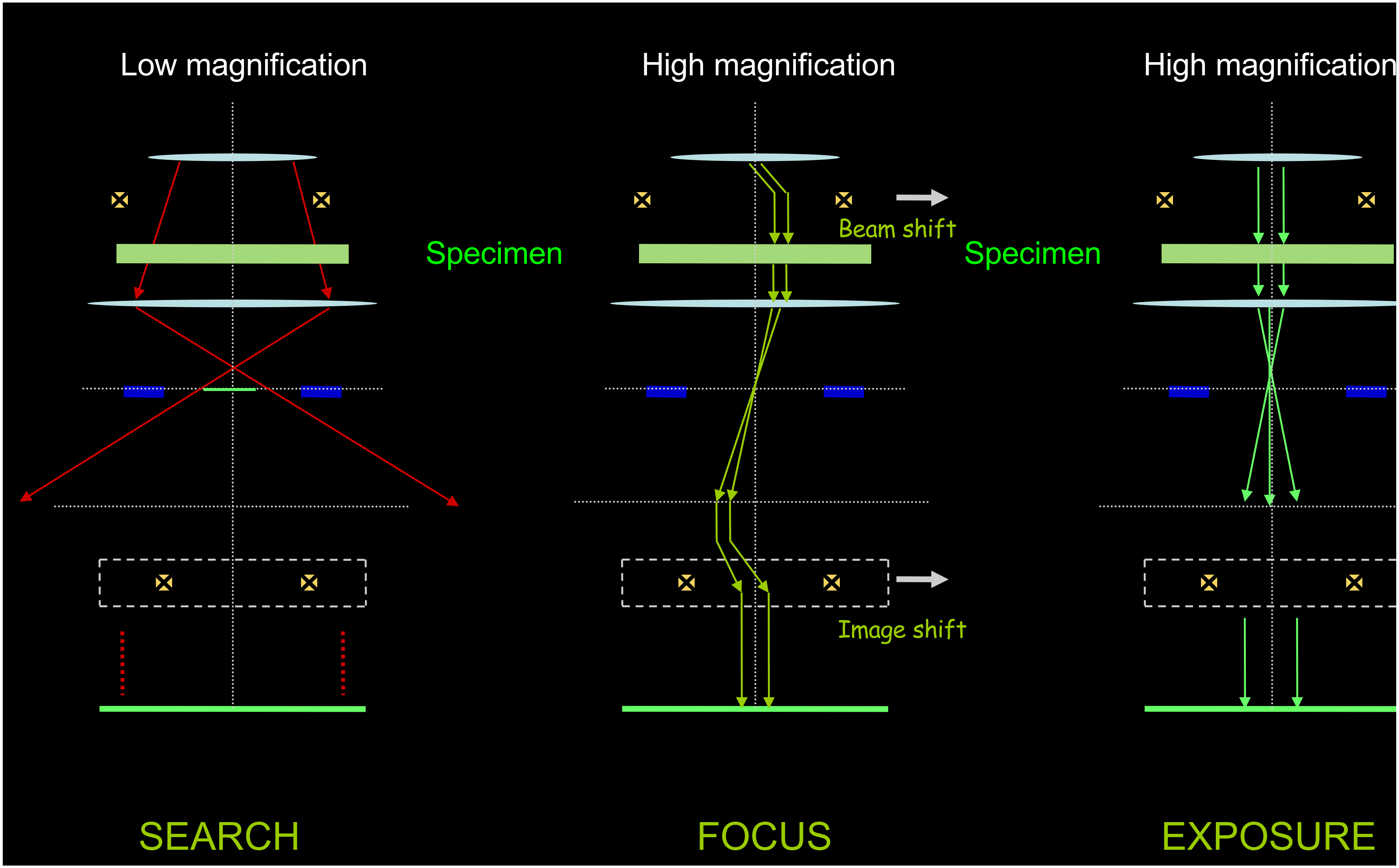

Principle of low-dose microscopy

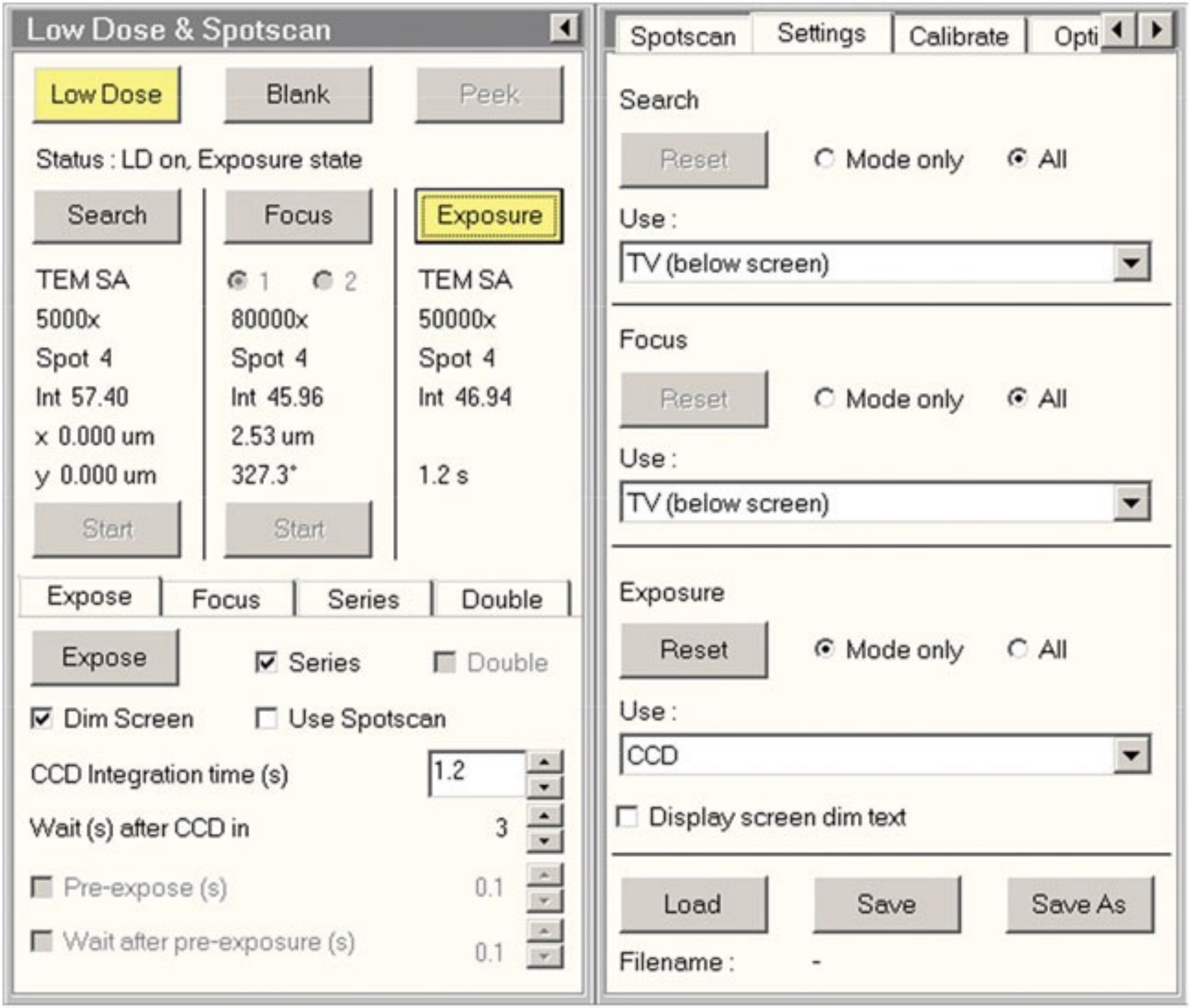

Cryo holder

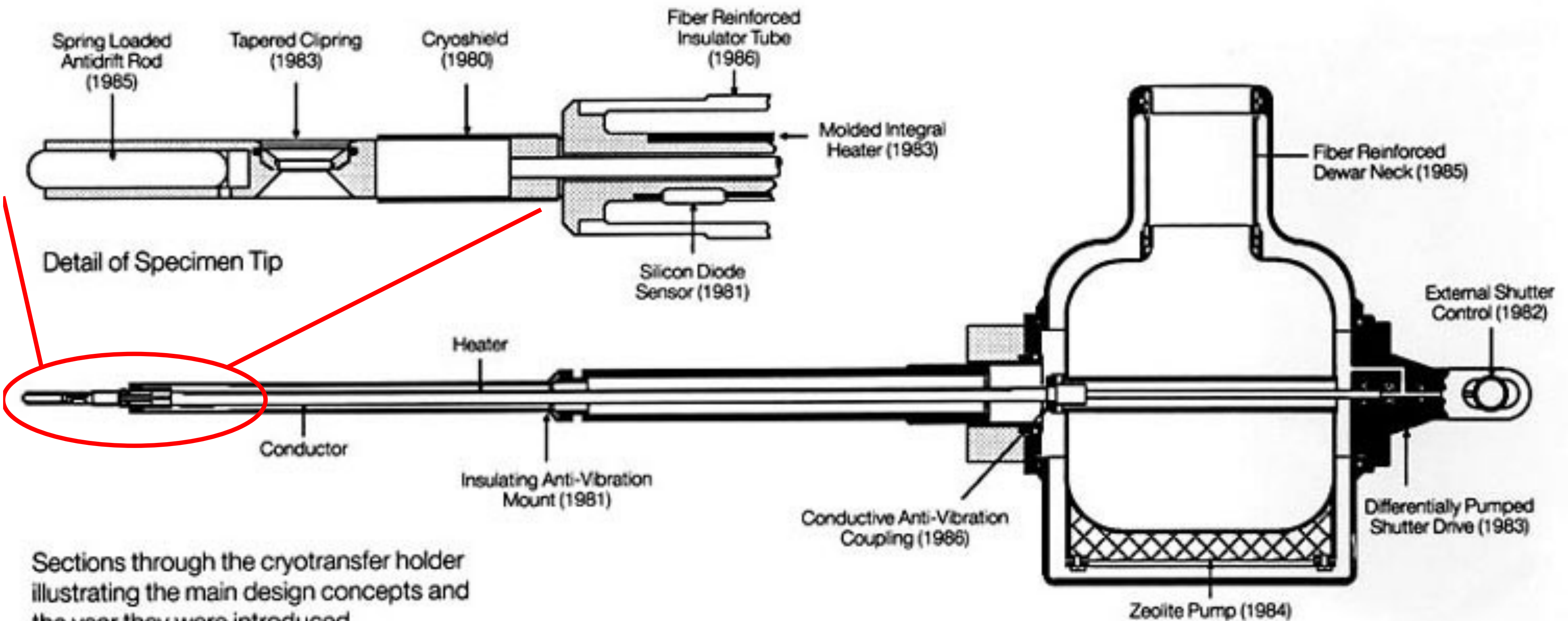

Sections through the cryotransfer holder illustrating the main design concepts and the year they were introduced.

Ice forms

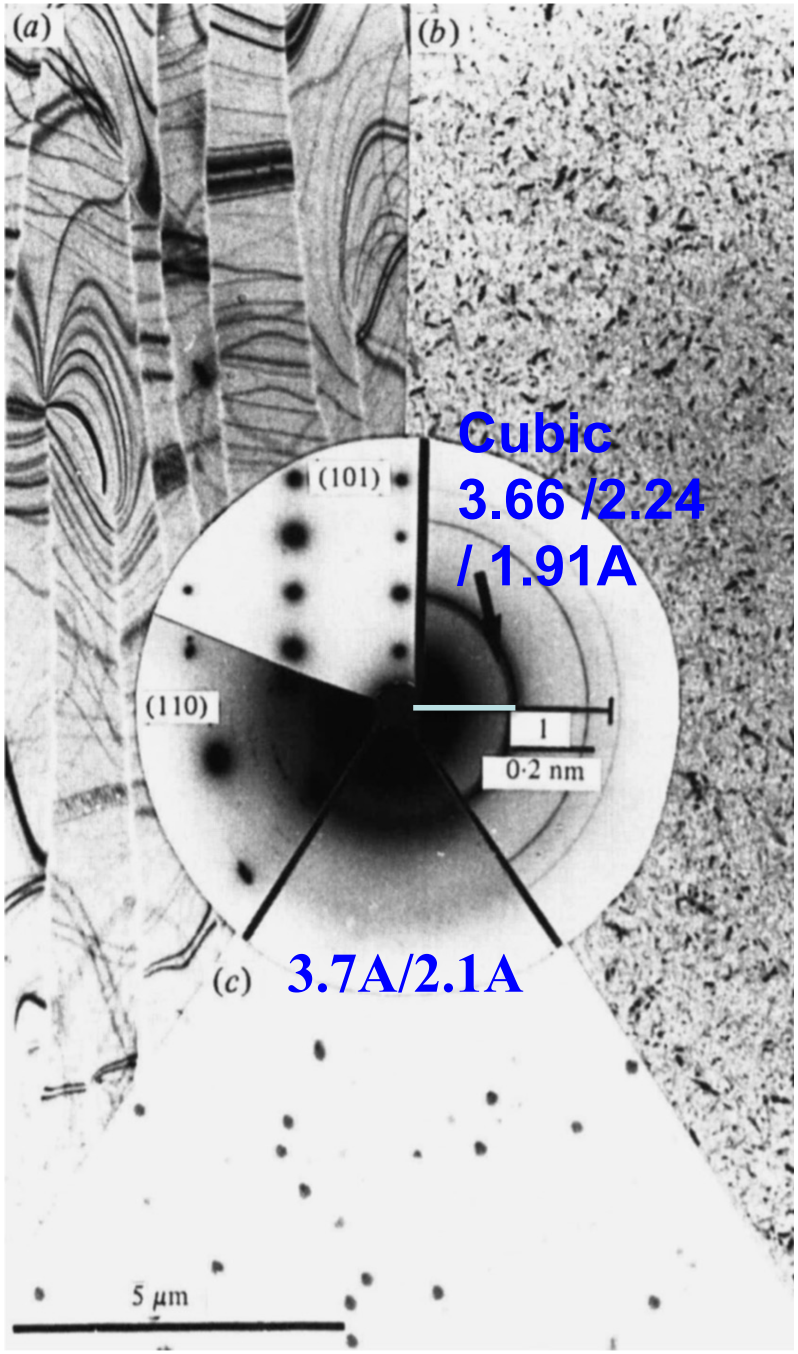

Fig. 5. Typical images and electron diffractograms of three forms of solid water observed in the electron microscope. The direct images and their diffractograms are all printed at the same scale, (a) Hexagonal ice obtained by **rapid freezing** of a water layer on a carbon film. The diffractograms, obtained from other specimens, show the (110) and (101) plane, (b) Cubic ice obtained by **warming a layer of vitreous water** obtained by condensation. The shoulder on the (111) reflection, possibly indicating the presence of a small amount of hexagonal ice, is marked by an arrow, (c) Vitreous water obtained in the microscope, by **condensation of vapour on a cold carbon film** supporting **polystyrene spheres**.

Table 2. *Main reflections in the electron diffractogram of the various forms of ice at −160 °C*

Hexagonal	Cubic	Vitreous	*d* (nm)	Intensity
100	—	—	0·389	Very strong
	—	First maximum	0·370	Very strong
002	111	—	0·366	Strong/very strong
101	—	—	0·343	Strong
102	—	—	0·266	Weak
110	220	—	0·224	Medium/medium
	—	Second maximum	0·214	
103	—	—	0·207	Medium
200	—	—	0·194	Very weak
112	311	—	0·191	Weak/weak
201	—	—	0·188	Very weak
202	—	—	0·172	Very weak

Ice contamination

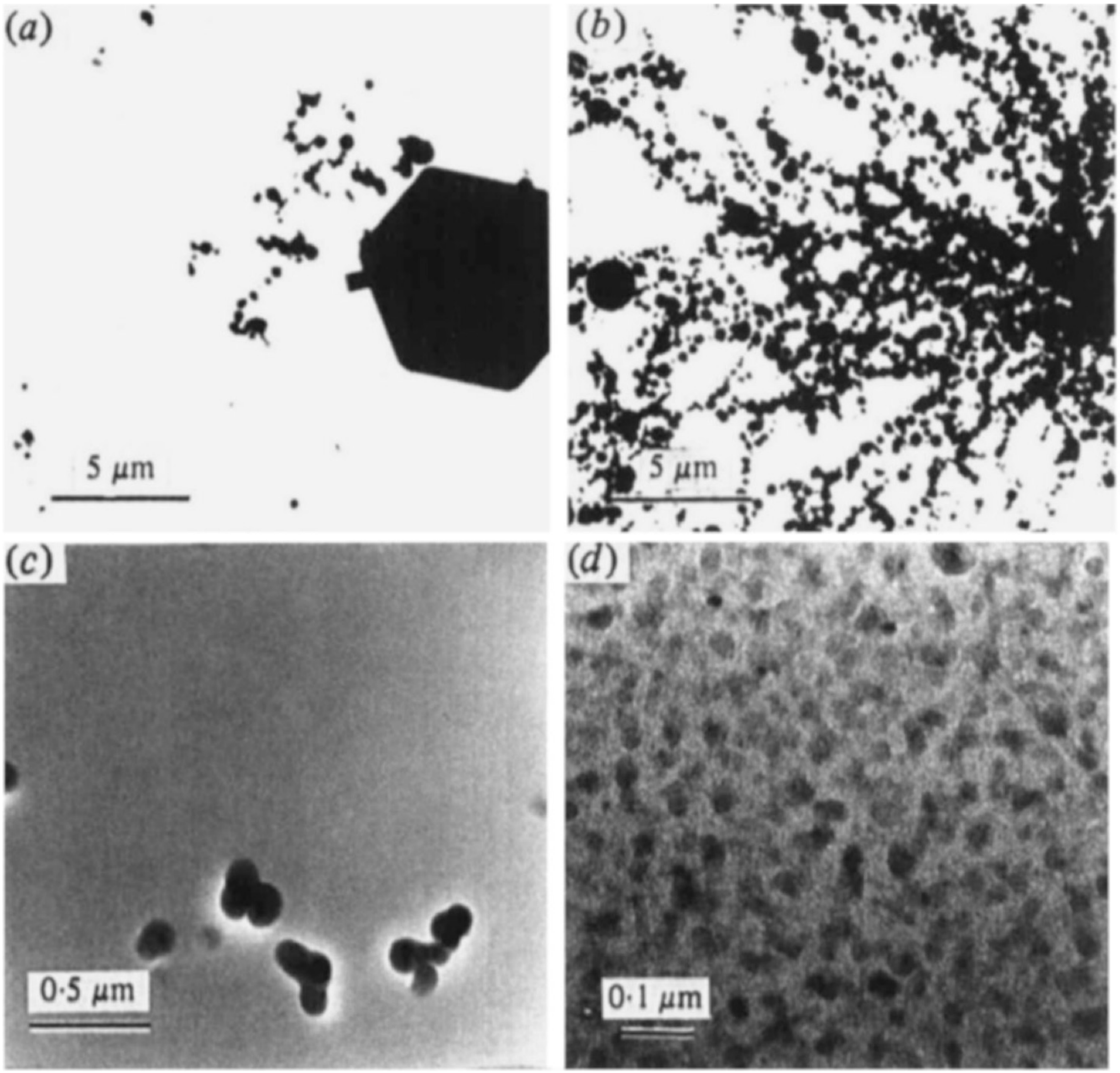

Fig. 32. Various forms of contamination on the specimen, *(a)* **Hexagonal ice** crystals **formed in humid air** and deposited during preparation of the specimen (in particular in the cryochamber of the microtome) and during transfer, *(b)* Agglomerate of **hexagonal ice** crystals **formed by humid air condensing on liquid nitrogen**, *(c)* Layer of **vitreous water deposited in the microscope**, on a thin vitrified film. **Hexagonal ice** crystals deposited on the specimen have been shadowed, thus revealing the contaminating layer and demonstrating that the water molecules came predominantly from one direction, *(d)* Crystals of **cubic ice** formed by deposition of water vapour in the microscope in a similar but **more rapid way** than in *(c)*.

Dubochet, J., Adrian, M., Chang, J. J., Homo, J. C., Lepault, J., McDowall, A. W. & Schultz, P. (1988). Cryo-electron microscopy of vitrified specimens. Quarterly Reviews of Biophysics, 21(2), 129-228.

Carbon film growth and transfer

- Grow carbon film on mica sheet, then float the continuous carbon onto TEM grids
- Coat commercially available TEM grids with fresh carbon

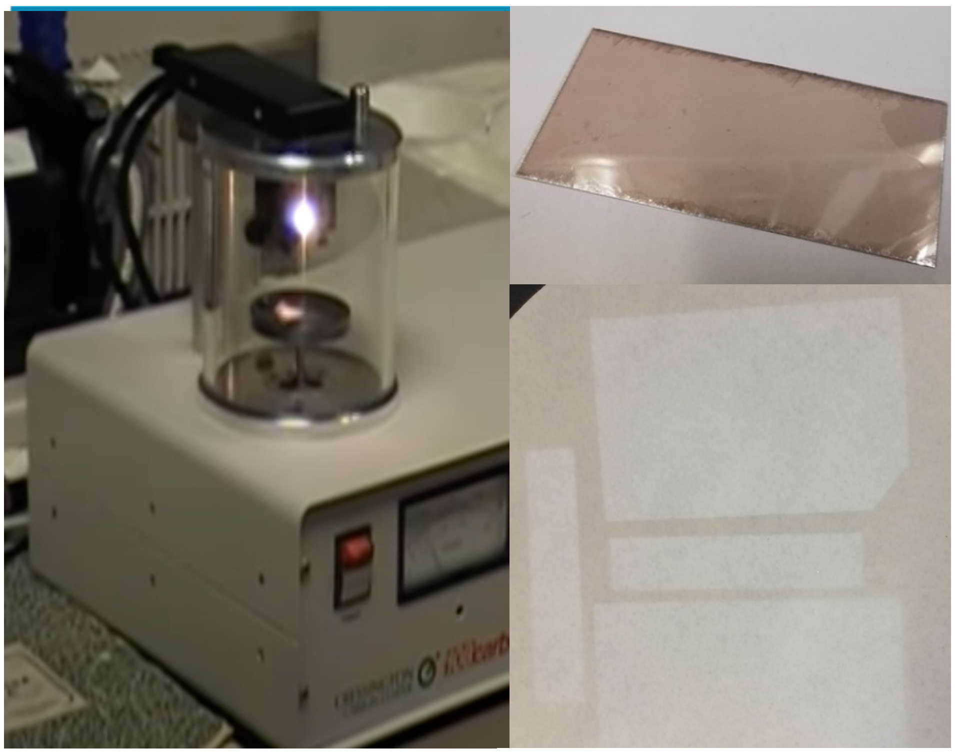

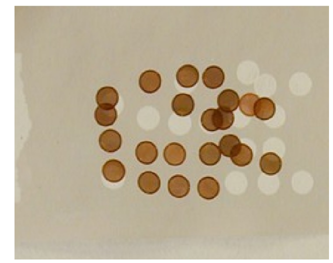

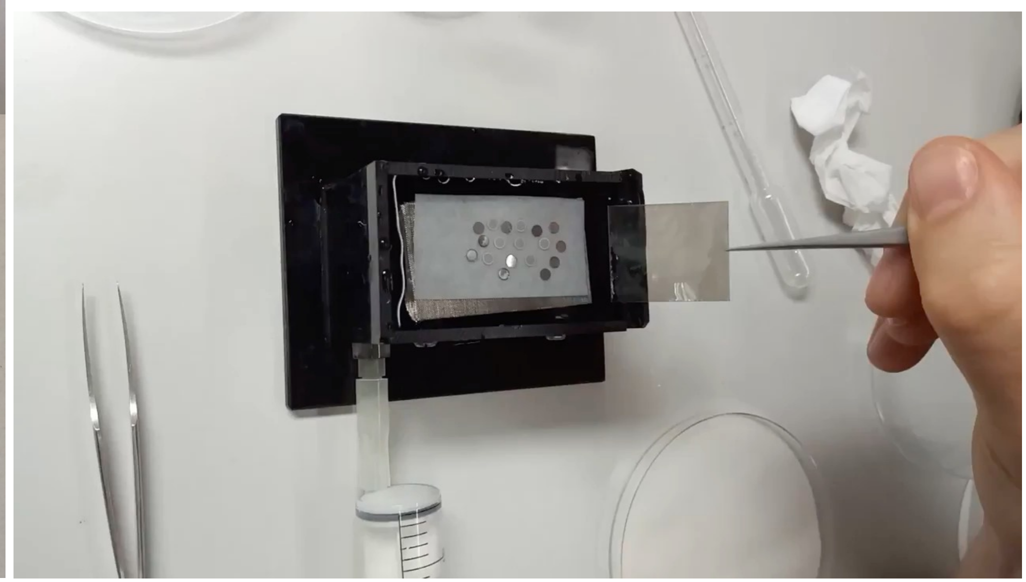

[Carbon Coating Grids Electron Microscopy SJDC Dr. Jon Krupp - YouTube]